

MASSACHUSETTS INSTITUTE OF TECHNOLOGY  
HAYSTACK OBSERVATORY

WESTFORD, MASSACHUSETTS 01886

Telephone: 617-715-5400

November 6, 2018

To: Distribution  
From: Brian E. Corey  
Subject: **Notes on KOKEE20M phase cal**

These notes summarize my investigation into the quality of the phase cal signal at KOKEE20M. It was instigated by Laura La Porta's question last March whether the phase cal is good enough to use in fringe-fitting, in place of the manual phases that have been used (at my recommendation) for over two decades.

### 1. Conclusions first

I find that phase cal is sufficiently free of spurious effects that it can be used for fringe-fitting. Contamination by spurious signals causes worst-case MBD errors of a few ps rms. Unusual scan-to-scan jumps in phase cal phases in some channels appear to originate in the main signal path; fringe-fitting Kokee data with multitone phases corrects for these jumps. Switching from manual phases to multitone phases may result in a shift of a few mm in the solved-for height of the antenna due to elevation-dependent instrumental delays that could not be corrected for when fringe-fitting with manual phases. Certain phase cal tones should be masked out in fourfit when calculating multitone phases.

### 2. Data analyzed

All data are from the most recent R&D sessions involving Kokee that have been processed at Haystack: RD1701, RD1702, RD1706, RD1707, and RD1804. The phase cal (pcal) behavior was similar in all five sessions; in these notes I focus on RD1707. Because Kokee observed exclusively with Wettzell during the RD17xx sessions, it never pointed to the south. Only during RD1804 did Kokee point south.

### 3. Multitone phases and amplitudes

Scan-averaged multitone phases and amplitudes were calculated in fourfit from the unmasked pcal tones and then extracted in aedit. Because certain tones appear to be corrupted (see section 4), the following tones were masked out using the fourfit keyword *pc\_tonemask*: the 5<sup>th</sup> tone (4.01 MHz at baseband) in S-band USB channels, the 3<sup>rd</sup> and 8<sup>th</sup> tones (2.01 and 7.01 MHz) in X-band USB channels, and the 5<sup>th</sup> tone (4.99 MHz) in the X06LR. (See Table 1 on page 7 for channel labels.) In all cases except X06LR, the RF frequencies of the masked tones are integer multiples of 5 MHz.

#### 3.1 Temporal variations in phases and amplitudes

Plots of RD1707 multitone pcal time series for individual frequency channels are presented in the first four figures: phase in **Figure 1**, amplitude in **Figure 2**, phase differences between channels in **Figure 3**, and amplitude ratios between channels in **Figure 4**.

In addition to the uninteresting slow drifts in phase in common across all channels within a band (**Figure 1**), noteworthy time variability is present on three time scales in the figures:

- (a) Slow drifts over many hours of up to  $40^\circ$  pk-pk in phase differences between adjacent channels, with an overall shape similar to the undifferenced phase time series.
- (b) Variations on time scales from a half hour to a few hours in phase differences (generally  $<5^\circ$  pk-pk) and in amplitude ratios (generally  $<6\%$  pk-pk).
- (c) Bimodal variations from scan to scan, seen most easily in phase differences, e.g., S2-S1 and X3-X2, with jumps of up to  $2-3^\circ$  (and as much as  $6^\circ$  in S2-S1 during the first few hours).

The first two are the subjects of the next two subsections, while the third is deferred to section 5.

### 3.2 Slow drifts in channel phase differences

Diurnal, thermally driven variations in instrumental delay generally cause the largest temporal variations in pcal phase and in phase differences between channels, and Kokee is no exception. Such variations scale with frequency difference between channels. Their effect was removed from the pcal phases by constructing a “band model” for each epoch in each band, then subtracting the model value from each phase point. The band model is a straight line fit to the 6 or 8 pcal phases vs. frequency, after first subtracting the phase of the first scan from the phase time series for each channel. The slope of the line is sometimes referred to as pcal delay. (The band model is the pcal equivalent of estimating the residual MBD and fringe phase at the reference frequency in fourfit.) The pcal phase differences after band model correction are plotted in **Figure 5**.

While the slow, quasi-diurnal variations are generally smaller in Figure 5 than in Figure 3, they are still present in Figure 5, particularly at X-band. These appear to be due primarily to BBC LO phase drifts, as shown by comparing pcal and fringe phases: In **Figures 6 and 7** are plotted the time series of the channel pcal phases after subtracting the band model. (The points in Figure 5 are differences between the channel phases in Figures 6 and 7.) If the temporal variations in Figures 6 and 7 are caused by instrumental phase variations that also affect the fringe phases, fringe-fitting the data with manual phases for Kokee should lead to similar variations in the fringe phases, whereas fringe-fitting with multitone pcal should remove the variations. As shown in **Figures 10 and 11**, fringing X-band with manual phases yields channel fringe phase time series that match well the large-scale (in time and magnitude) pcal phases in Figure 7, whereas fringing with multitone pcal produces fringe phases with no significant (at the level of the fringe phase errors) variations. S-band fringe phases from manual and multitone fringing shown in **Figures 8 and 9** are very similar, as expected, given the small size of the phase variations in **Figure 6**.

### 3.3 Channel phase variations on time scales of a half hour to a few hours

Phase variations on time scales of roughly a half hour to a few hours in Figure 7 are  $<5^\circ$  pk-pk – too small to be seen in the manual-vs.-multitone fringe phase comparison. Other methods, including examining plots of pcal amplitude time series and of amplitude or phase vs. phase, must be used to tell whether the phase variations reflect instrumental delay/phase variations in the main (i.e., quasar) signal path or flaws in the pcal signal itself (e.g., spurious signals).

In the absence of spurious signals and equipment problems, pcal amplitude should not be affected by instrumental delay/phase variations. The fact that the pcal amplitude ratios in **Figure 4** vary on similar time scales to the phase differences in **Figure 5** hints of spurious signal contamination. The sizes of the variations in the two figures are also generally consistent with each other. For example, for channels X6

and X7, the amplitude ratio varies by up to 7% pk-pk, which implies a phase variation of 0.07 radian, or 4°, as observed in the phase differences.

**Figure 12** is a set of standard amplitude-vs-phase plots commonly used to look for evidence of spurious signals. The upper envelopes of the S1 and S2 amplitudes show the 180°-period sinusoid characteristic of image-type spurs. The sinusoid half-amplitudes of ~3% and ~1.5% imply phase errors of  $\pm 1.7^\circ$  and  $\pm 0.9^\circ$ , respectively. In turn, these phase errors will cause MBD errors of approximately  $\pm 20$  ps and  $\pm 7$  ps, or only  $\pm 1.5$  ps and  $\pm 0.5$  ps in the ionosphere-free delay. Variations in the other S-band channels are smaller than in S1 and S2.

It is harder to make sense of the X-band amplitude-vs-phase plots, particularly in the higher-numbered channels. In part this is due to the scatter in amplitudes caused by scan-to-scan variations in  $T_{\text{sys}}$ . Multiplying each amplitude by the square root of  $T_{\text{sys}}$  from the Field System log reduces the scatter for most points, as seen in **Figure 13**. But some channels such as X6-X8 still exhibit unusual patterns that hint of structure not periodic over 360°. **Figure 14** is the same as Figure 13 except that now the abscissa is the *connected* phase of the first channel in the band. In several channels are clear systematic amplitude variations not periodic over 360°. (Figure 15 shows the X-band amp-vs-phase variations even more clearly, although with the disadvantage that, by dividing each amplitude by the mean over all channels, each plot is contaminated by systematic variations in the other channels.) The cause of the variations is unknown, but similar sorts of nonperiodic (or periodic over phase spans other than 180° and 360°) variations at other stations have been traced to crosstalk between two pcal signals, e.g., S and X at IF frequencies.

The largest amplitude variation is  $\sim \pm 4\%$  in X8, which if due to a spurious signal would result in a phase error of  $\pm 2^\circ$ , or a MBD error of  $\pm 4$  ps.

Complementary to the amplitude-vs-connected-phase plots is **Figure 16**, where the pcal phase residual to the band model (i.e., the points in Figures 6 and 7) is plotted vs. connected phase of the first channel. Again, care must be taken in interpreting these plots, as variations in other channels bleed over into each plot because of subtracting the band model. That said, on top of the scan-to-scan variations seen in some channels, there are distinctive systematic features in some channels. Ignore the quasi-linear trends in channels like X4, X5, and X8, as these correspond to the LO drifts of section 3.2 and do not reflect a pcal error. Instead focus on the wiggles on top of the linear trends. The largest wiggles are  $\sim \pm 2^\circ$  in X8 – a result consistent with the estimate from the amplitude-vs-phase plots.

Summing up: the worst-case pcal phase errors estimated from plots of amplitude or of phase difference relative to band model vs. phase are  $\pm 2^\circ$  in S1 and X8, with corresponding ionosphere-free delay errors of  $\pm 2$  ps and  $\pm 4$  ps, respectively. The magnitude of these phase variations is consistent with that of the variations in Figures 5-7 on intermediate time scales. It appears then that the latter are in fact due to pcal phase errors and not due to BBC LO phase variations, for instance. Phase errors within a 1-hour span are typically much less than  $\pm 2^\circ$ , however, so the added noise from pcal errors will usually be much less than  $\pm 4$  ps over the clock interval in a geodetic solution.

#### 4. Phases and amplitudes of individual pcal tones

Some aspects of the multitone pcal quality can also be assessed by examining the amplitudes and phases of the individual pcal tones. These were calculated by a non-HOPS program from the data in type-309

station files. **Figures 17 and 18** display the tone amplitudes vs. time and phase. Tone 5 in S03UR (S4) and X06LR (X1 LSB) and tones 3 and 8 in most X-band USB channels behave anomalously compared with the other tones in each channel.

These differences are more pronounced in **Figures 19 and 20**, where each tone amplitude has been divided by the mean amplitude over all tones in the channel except for those tones masked out (as indicated by a large 'X' across the panel). The masked tones were specified at the beginning of section 3.

With various tones masked out, a “channel model” similar to the band model of section 3 was fit to the phases of the unmasked tones in each channel for each epoch. The intercept of the best-fit line at the mid-channel frequency is the multitone phase of fourfit (‘PC phase’ on a fringe plot), and its slope is the multitone delay (‘PC delay’). In **Figure 21** are time series plots of the model phase and delay. The bimodal, scan-to-scan delay variations in some channels imitate the multitone phase variations of Figures 6 and 7 well in some cases, poorly in others.

**Figures 22 and 23** show the difference between tone phase and channel model value plotted against time and phase, respectively. Such plots aid in identifying tone-dependent spurious signals but are insensitive to common-mode spurious signals. There are obvious systematic differences in phase behavior among tones within each channel. Aside from the masked tones, however, no tone exhibits systematic phase variations larger than  $\pm 1^\circ$ , so the pcal errors identified in section 3 cannot be due to “bad actor” tones.

## 5. Scan-to-scan multitone phase and delay variations

The multitone phase and delay jumps from scan to scan are most peculiar. They are present in some channels but not others. In a given channel, they may be present for hours at a time, then disappear for hours. Phase jumps are sometimes synchronized between channels within a band, other times not, but there is little synchronization between bands; delay jumps are poorly synchronized within and between bands. The magnitude of the delay or phase jumps varies from channel to channel but it tends to be stable for a given channel.

Where lies the fault causing the jumps? The bottom panels in **Figures 24 and 27** show that the phase “state” depends on antenna elevation. This points to the receiver, or perhaps an antenna cable, although a backend problem isn’t entirely ruled out, as the backend could conceivably be responding in a binary fashion to the input IF level, which varies with elevation. A problem in the pcal generator is extremely unlikely as the jumps should be present in all channels, and the magnitude of the phase jumps should scale with RF frequency. Frequency-dependent contamination of pcal by spurious signals, either before or after pcal injection into the main signal path, is a possibility, as is a fault in a component common to both the S- and X-band signal paths through the receiver (e.g., a power supply).

For the purposes of this note, what matters most is whether the jumps are a reflection of a fault in the pcal signal or in the non-pcal equipment. If the former, applying pcal in fourfit will degrade the MBDs, while if the latter, it will improve them.

Based on the information presented in Figures 24-29 and Table 2 (page 37), and on similar tests run on RD1706 data that yielded similar results, it appears the fault is not in the pcal signal, and that applying pcal in fourfit is a good thing.

**Figures 24-26** concern the jumps in S1 phase, as reflected in the S2-S1 phase diff, during the last 9 hours of RD1707. Different plot symbols indicate whether the difference between S2-S1 and the green dotted line in the top left panel of each figure is positive or negative. The top right panel in Figures 25 and 26 is the S2-S1 fringe phase difference time series when Kokee is fringed with manual or multitone phases, respectively, while the lower panel is fringe phase difference vs. pcal phase difference. The fringe phase scatter is much larger than the pcal phase scatter, but by averaging over all the scans, one can tease out (just barely) information about whether the jumps have pcal or non-pcal origins.

If the jumps are in the pcal signal, there should be no jumps in the fringe phase difference when Kokee is fringed with manual phases, while if the jumps are not pcal-related, fringe phase jumps should be present when Kokee is fringed with manual phases but not with multitone phases. From the second column of **Table 2**, the fringe phases do not jump when multitone phases are applied but they do with manual phases (although only by  $2\sigma$ ), by an amount consistent with the pcal phase jumps.

A similar check done on X3-X2 is illustrated in **Figures 27-29** and quantified in column 3 of the table. In this case, manual phase fringing results in a  $\sim 4\sigma$  detection of fringe jumps, again consistent with the size of the pcal jumps.

Note that, even if the conclusion that the fault is not in the pcal signal is wrong, the effect on MBD of the jumps observed in the RD17xx sessions is small enough not to be a serious issue. A  $2.5^\circ$  jump in S1 phase will shift the S-band MBD by 29 ps (for flat fringe amplitudes across frequency), or  $\sim 2$  ps in ionosphere-free delay. A  $2.8^\circ$  jump in X3 phase will shift the X-band MBD by  $\sim 2$  ps. The elevation dependence of the phase jumps would cause a shift of  $< 1$  mm in solved-for station height.

## 6. Dependence of pcal and cable cal delays on azimuth and elevation

Time series of pcal and cable cal delays for the 3 most recent sessions examined are plotted in **Figure 30**. While all the curves have qualitatively similar shapes, it is noteworthy that, for each session, the S- and X-band pcal delays differ significantly, and that cable delay varies far less than either pcal delay.

For the RD1707 and RD1804 plots in **Figures 31 and 32**, an 11-point running mean was subtracted from each time series, in order to accentuate scan-to-scan variations and, potentially, dependence on antenna pointing direction.

With far more scans per unit time, RD1707 provides the better test for elevation dependence. X-band pcal delay changes by  $\sim 10$  ps between  $10^\circ$  and  $60^\circ$  elevation in a roughly linear fashion, while S-band pcal delay changes by  $\sim 30$  ps over the same range in a nonlinear fashion. When a model comprised of a  $\sin(\text{el})$  term and a constant is fit to the X-band pcal delays, the coefficient of the  $\sin(\text{el})$  term is  $14 \pm 1$  ps, which corresponds to a height shift of  $\sim 4$  mm. Cable delay exhibits no elevation dependence to  $< \sim 1$  ps.

The facts of the last paragraph imply that the pcal elevation dependence originates in the receiver and/or downlink fiber and not in the pcal reference signal cable. In turn, this means that, if Kokee is fringed with multitone rather than manual phases, its solved-for height will shift by a few mm.

The limited azimuth data in Figures 31 and 32 suffice to rule out an azimuth dependence  $> \sim 5$  ps.

The pcal delay diurnal wanderings could conceivably originate in the pcal generator, as opposed to in non-pcal equipment. The fact that S- and X-band pcal delay time series differ somewhat argues for a non-pcal origin. Clock time series from geodetic solutions for data fringed with manual and multitone phases at Kokee might be useful for pinning down what drives the pcal delay drift, should anyone care.

**Figures and tables for “Notes on KOKEE20M phase cal”**

Each point in the figures represents the coherent average over a scan of a pcal- or fringe-related quantity.

In the notes and the associated figures, frequency channels are usually identified by shorthand versions of the channel labels used in correlator reports (column 1 in table below), but in Figures 17-23 the labels inserted by *difx2mark4* and present in the type-309 files (column 2) are used.

**Table 1. Frequency channel labels**

<i>Shorthand label</i>	<i>Type-309 label</i>	<i>Correlator report label</i>	<i>RF freq at DC edge (MHz)</i>
S1	S00UR	SR1U	2225.99
S2	S01UR	SR2U	2245.99
S3	S02UR	SR3U	2265.99
S4	S03UR	SR4U	2295.99
S5	S04UR	SR5U	2345.99
S6	S05UR	SR6U	2365.99
	X06LR	XR1L	8212.99
X1	X06UR	XR1U	8212.99
X2	X07UR	XR2U	8252.99
X3	X08UR	XR3U	8352.99
X4	X09UR	XR4U	8512.99
X5	X10UR	XR5U	8732.99
X6	X11UR	XR6U	8852.99
X7	X12UR	XR7U	8912.99
	X13LR	XR8L	8932.99
X8	X13UR	XRLU	8932.99

Kokee RD1707 pcal multitone phase time series

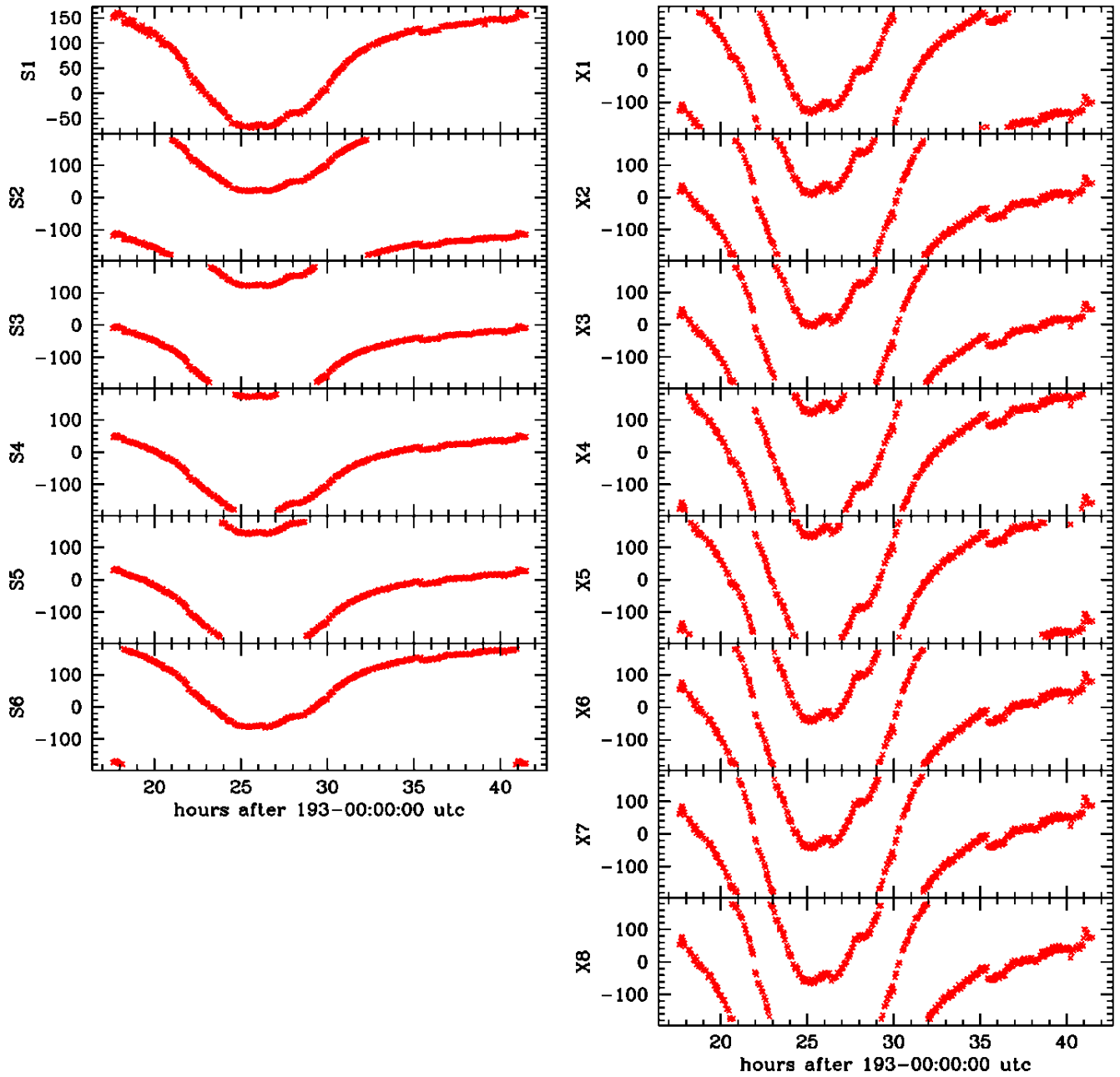


Figure 1. RD1707 S-band (left) and X-band (right) multitone pcal phase (deg) time series, by channel.

Koee RD1707 pcal multitone amplitude time series

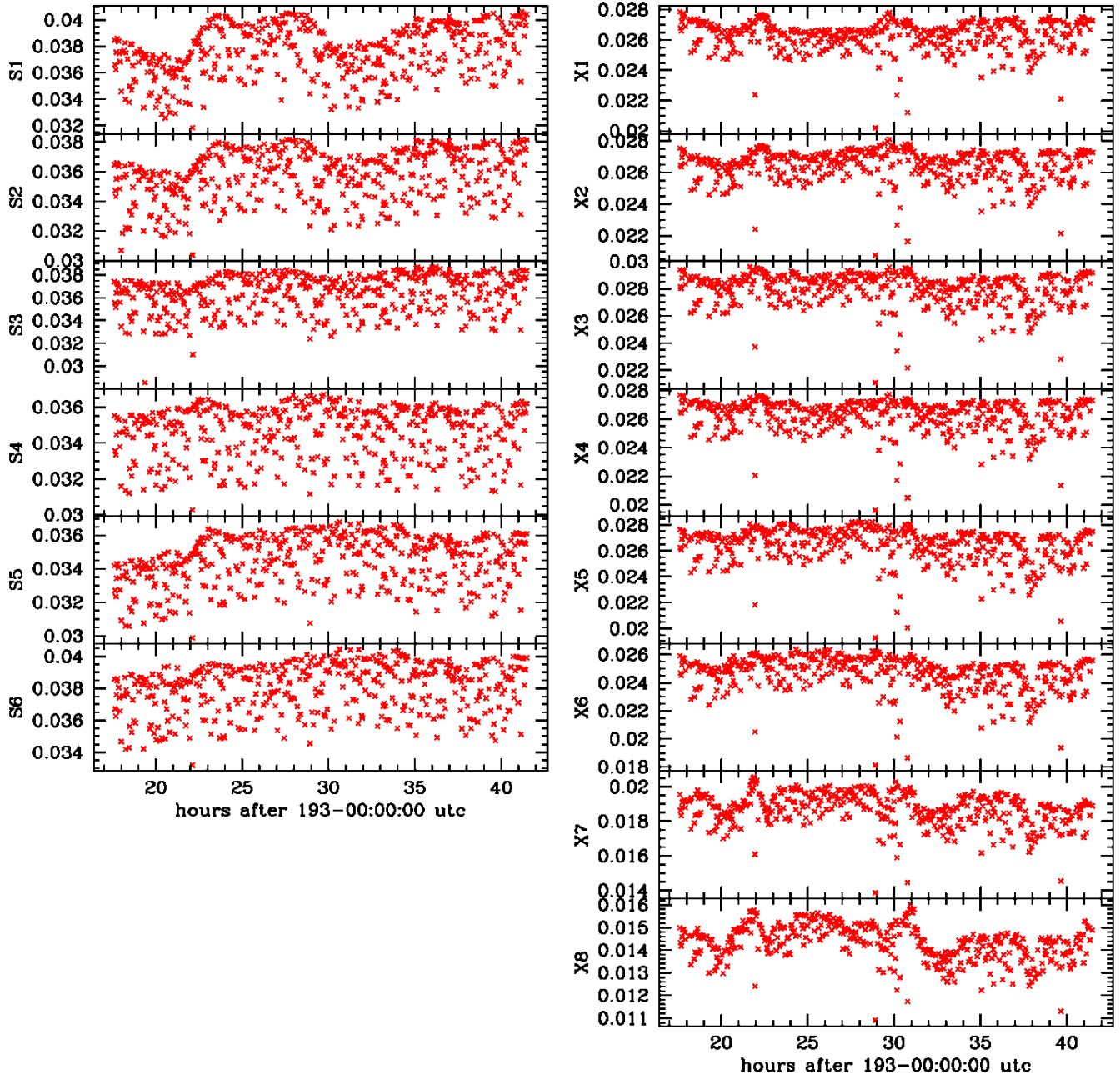
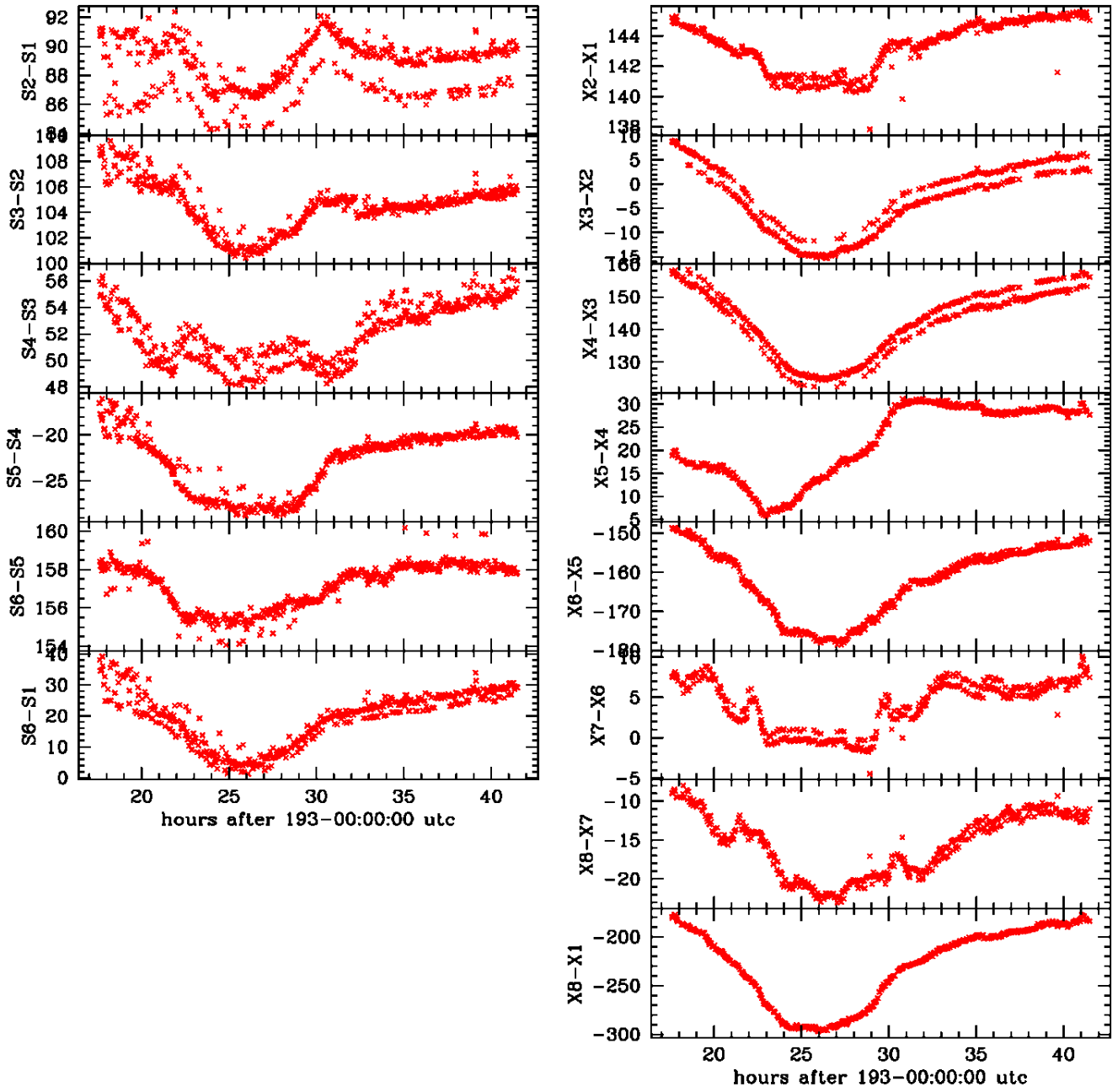


Figure 2. RD1707 S-band (left) and X-band (right) multitone pcal amplitude time series, by channel.

Kokee RD1707 pcal phase differences between channels



**Figure 3.** RD1707 S-band (left) and X-band (right) multitone pcal phase (deg) differences between adjacent channels and, in lowermost panels, between highest- and lowest- frequency channels.

Kokee RD1707 pcal amplitude ratios between channels

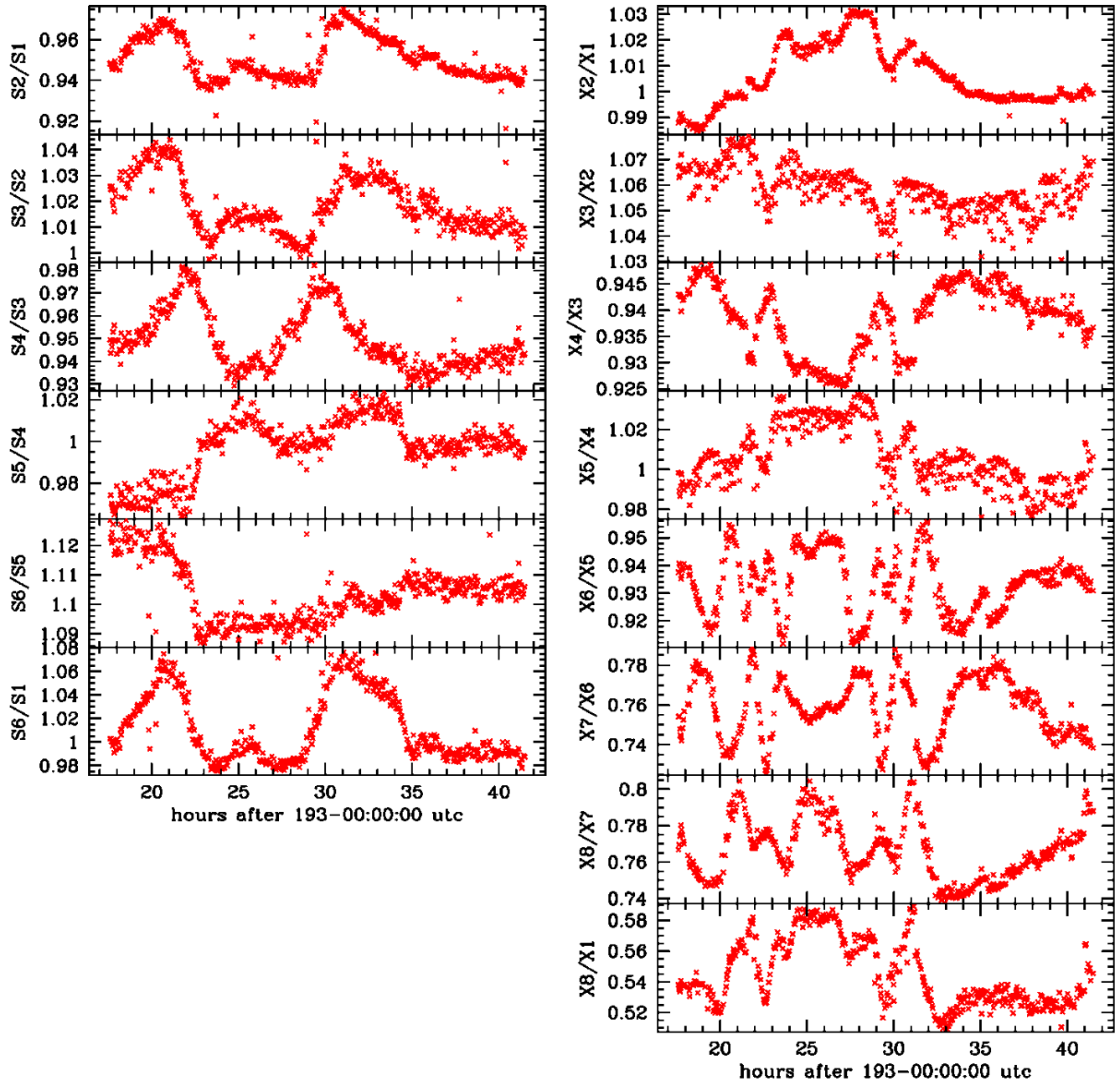


**Figure 4.** RD1707 S-band (left) and X-band (right) multitone pcal amplitude ratios between adjacent channels and, in lowermost panels, between highest- and lowest-frequency channels..

Koike RD1707 pcal phase differences between channels after subtracting band model

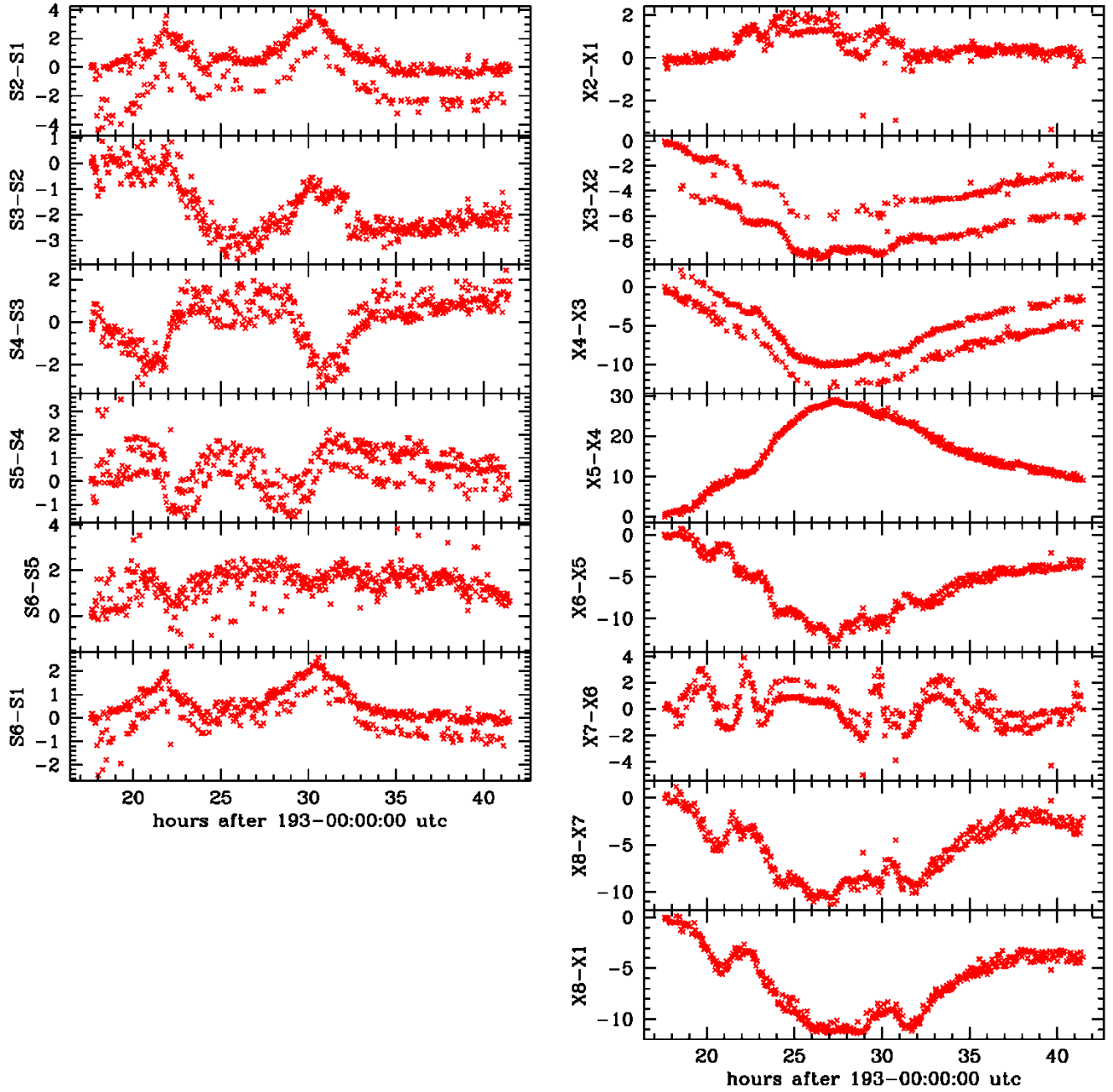


**Figure 5.** RD1707 S-band (left) and X-band (right) multitone pcal phase (deg) differences between channels after subtracting a “band model” from each phase. The band model for a given band is calculated at each epoch by fitting a straight line to the 6 or 8 channel phases vs. frequency, after first subtracting the phase of the first scan from the phase time series for each channel.

Kokee RD1707 S-band pcal phase residuals to band model

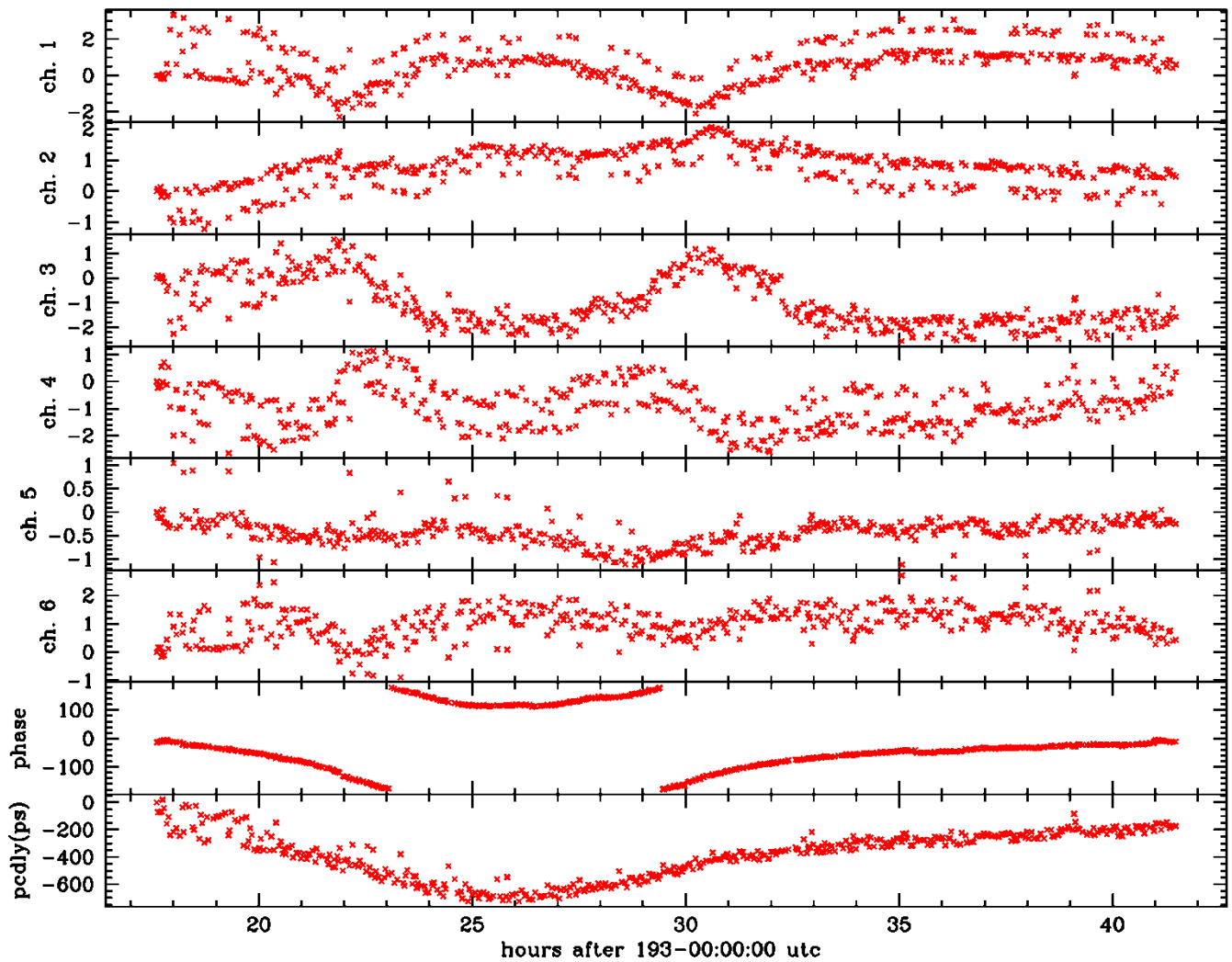


**Figure 6.** RD1707 S-band multitone pcal phase (deg) time series after subtracting the “band model” value from each phase. The band model for a given band is calculated at each epoch by fitting a straight line to the 6 or 8 channel phases vs. frequency, after first subtracting the phase of the first scan from the phase time series for each channel. Shown in the lower two panels are the phase (line intercept at frequency of lowest-frequency channel) and delay (line slope) of the band model.

Kokee RD1707 X-band pcal phase residuals to band model

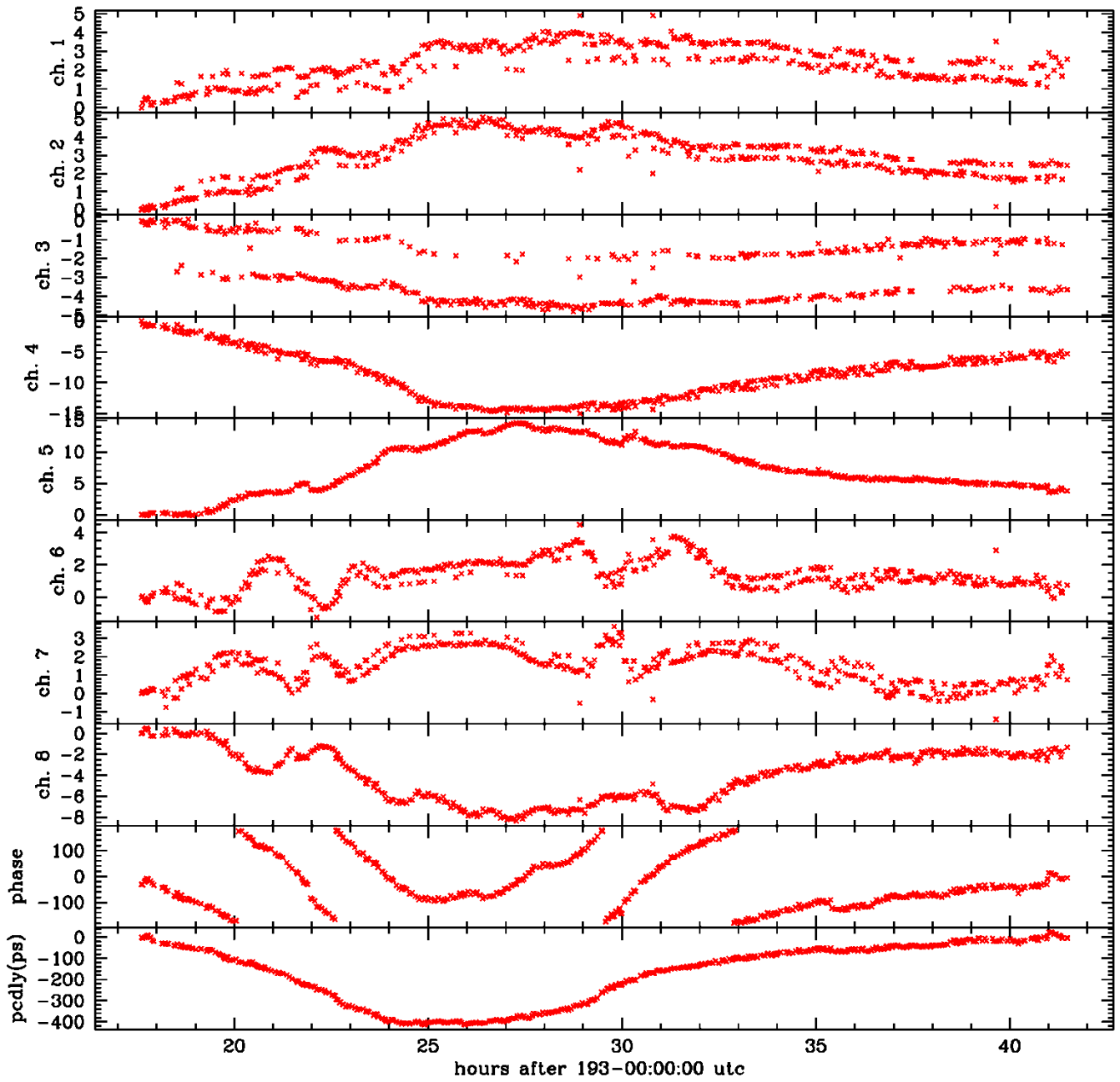
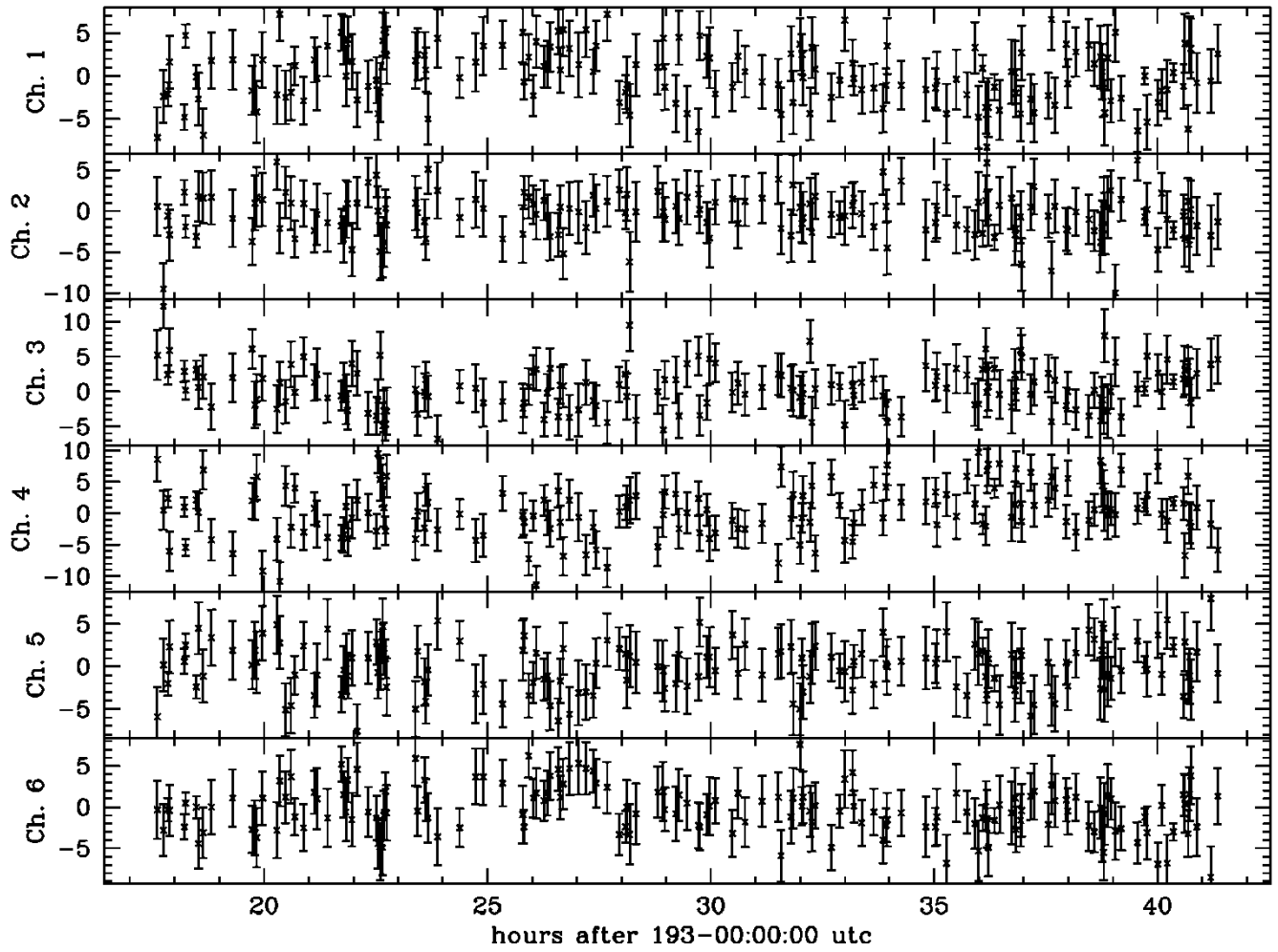


Figure 7. Same as Figure 6 except for X-band rather than S-band.

Kk-Wz RD1707 S-band channel fringe phases: Kk manual phases



**Figure 8.** RD1707 S-band residual channel fringe phase time series for KOKEE20M-WETTZELL baseline, relative to coherent average phase over all 8 channels, with **Kokee fringed with manual phases**. Only scans with SNR>30 are plotted. Error bars are approximately  $\pm 1\sigma$ .

Kk-Wz RD1707 S-band channel fringe phases: Kk multitone phases

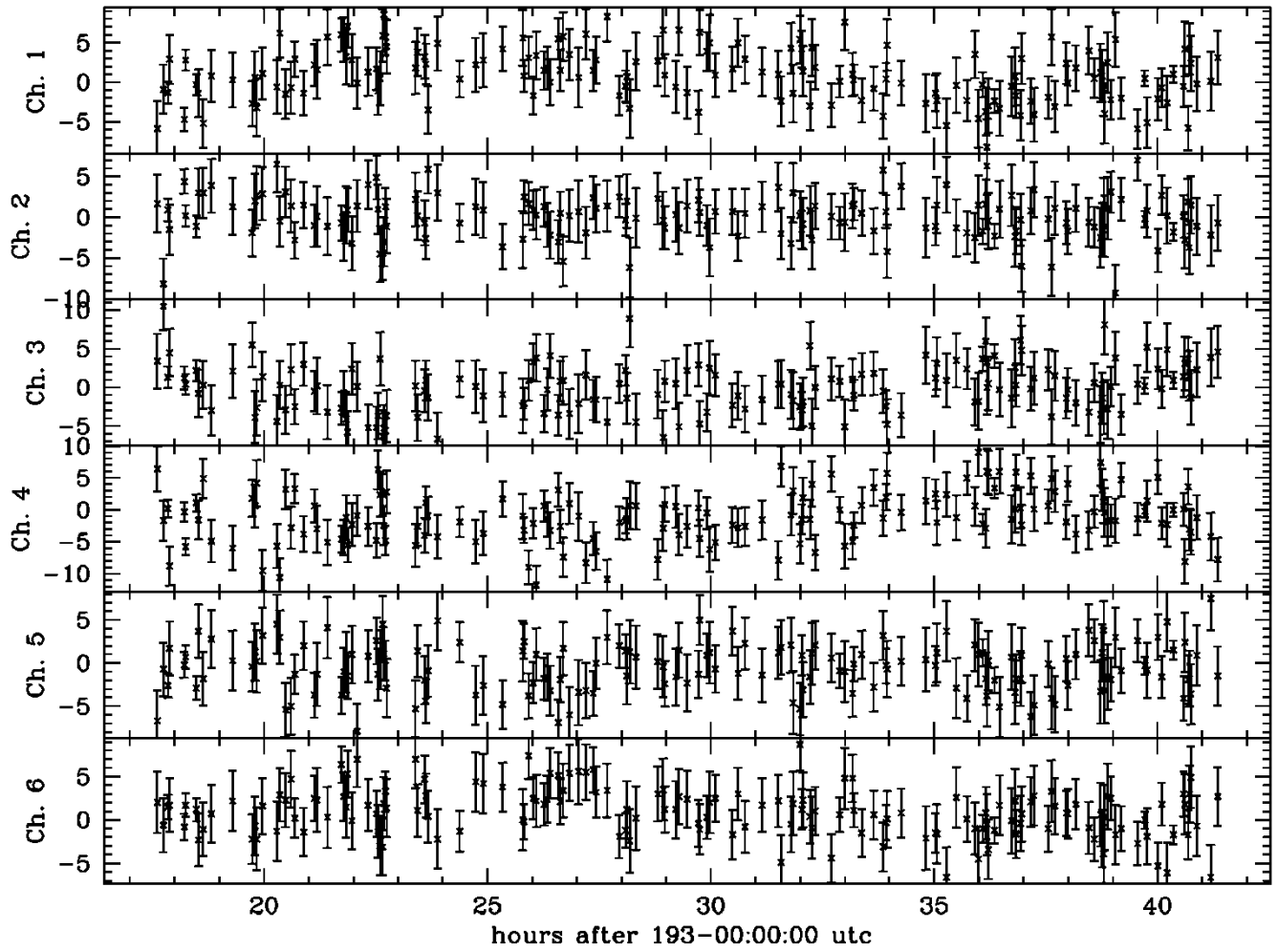


**Figure 9.** RD1707 S-band residual channel fringe phase time series for KOKEE20M-WETTZELL baseline, relative to coherent average phase over all 8 channels, with **Kokee fringed with multitone pcal phases**. Only scans with  $\text{SNR} > 30$  are plotted. Error bars are approximately  $\pm 1\sigma$ .

Kk-Wz RD1707 X-band channel fringe phases: Kk manual phases

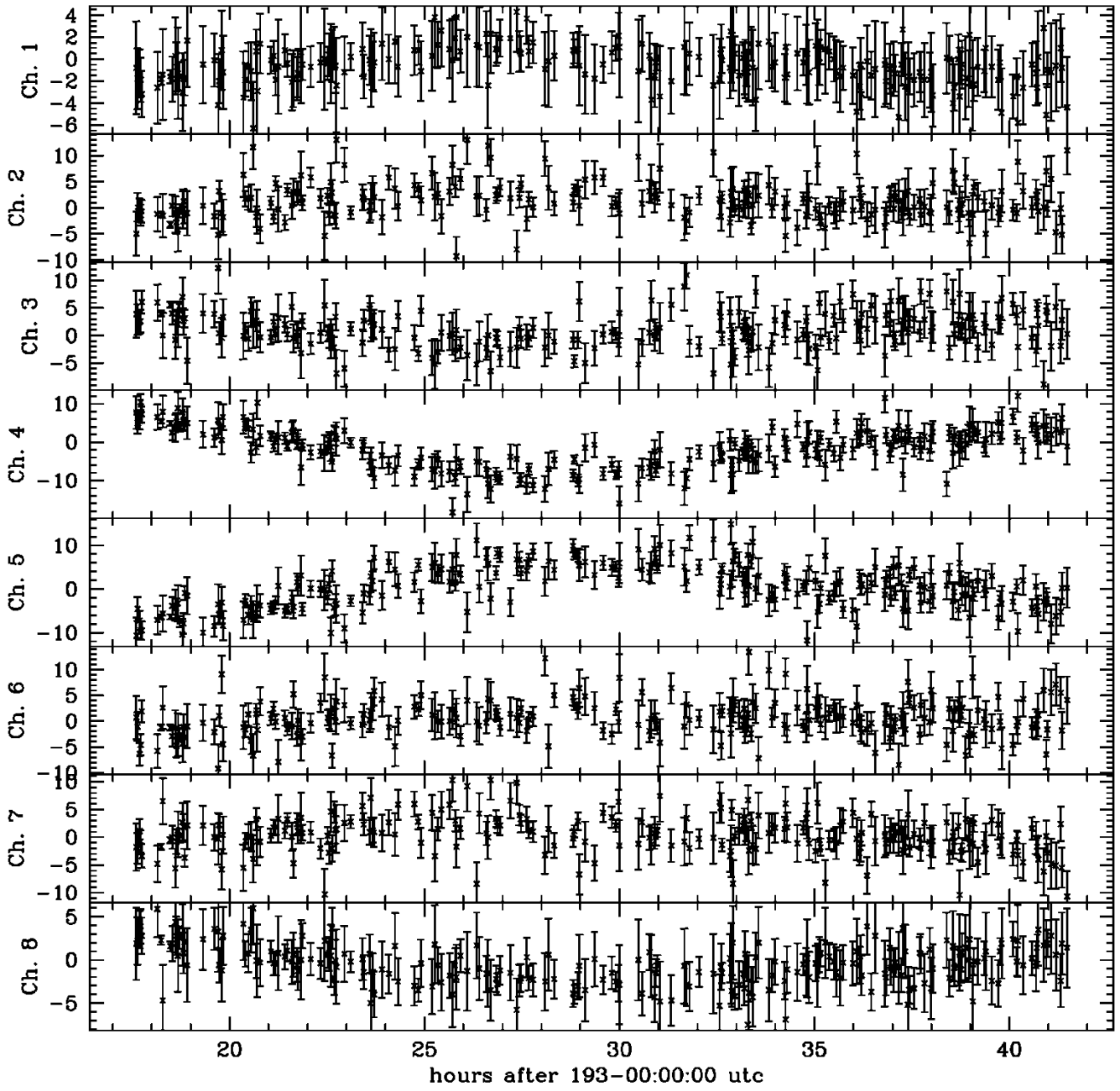


Figure 10. Same as Figure 8 except for X-band rather than S-band.

Kk-Wz RD1707 X-band channel fringe phases: Kk multitone phases

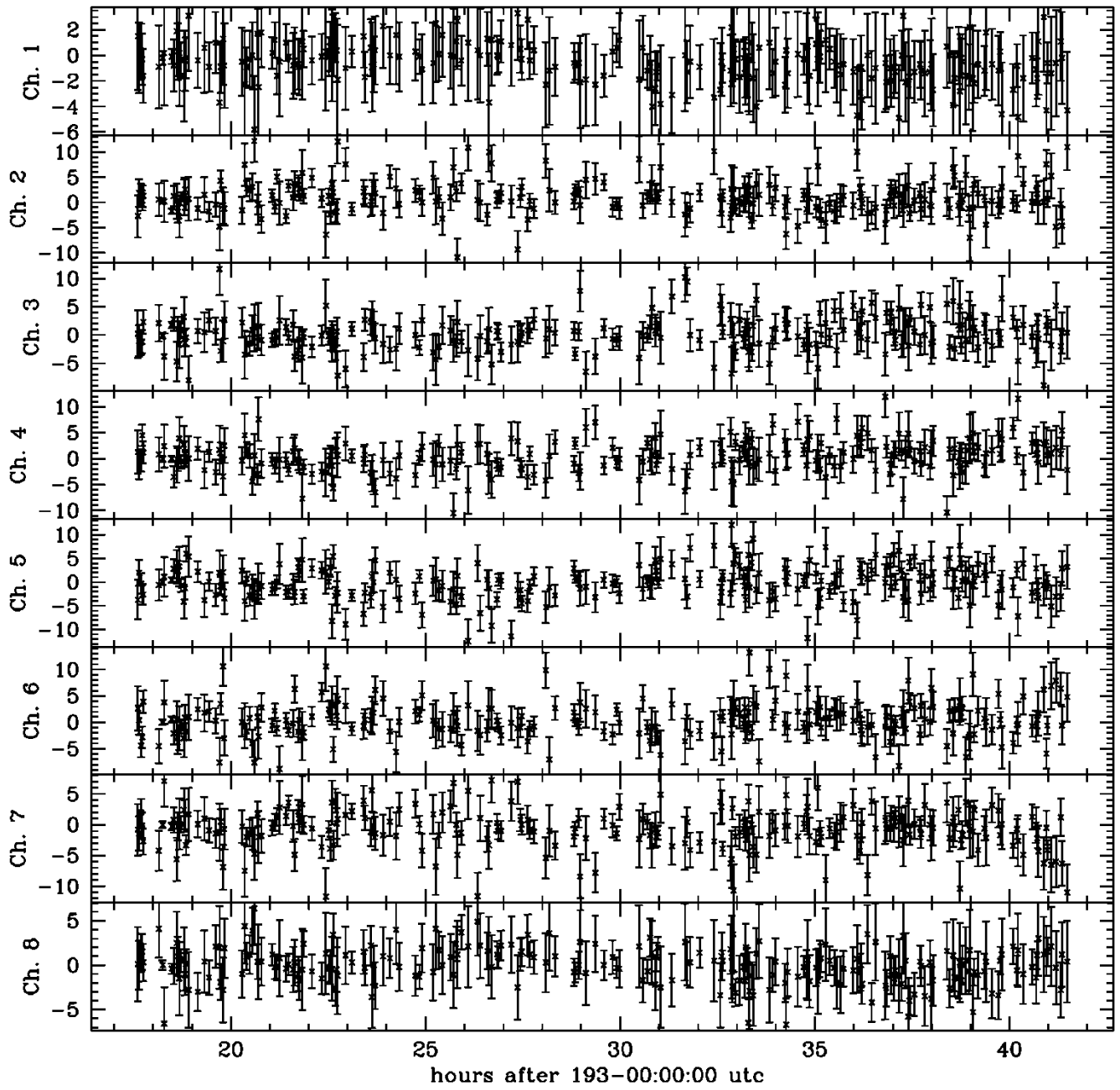


Figure 11. Same as Figure 9 except for X-band rather than S-band.

Koee RD1707 pcal multitone amplitude vs. phase

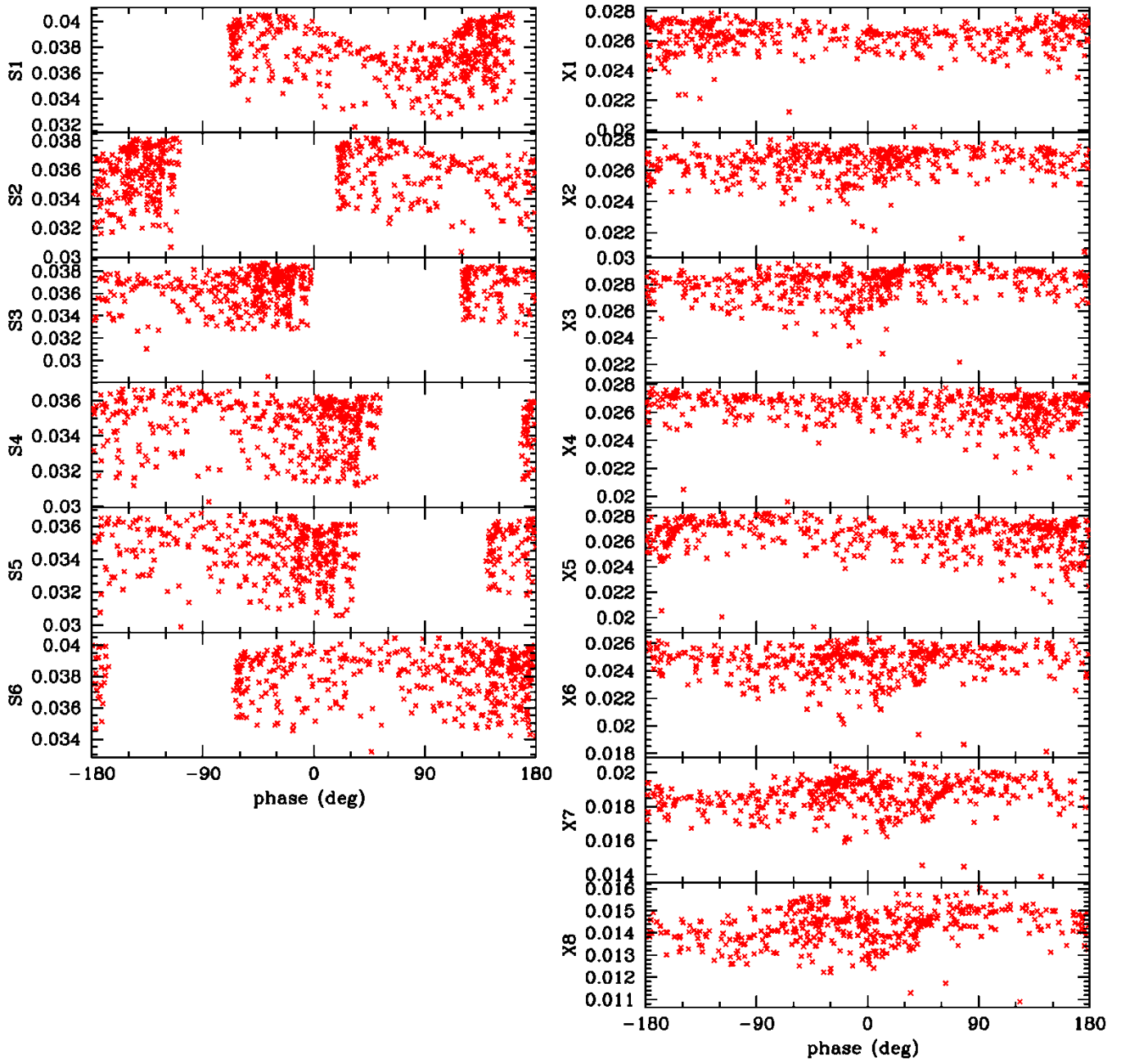
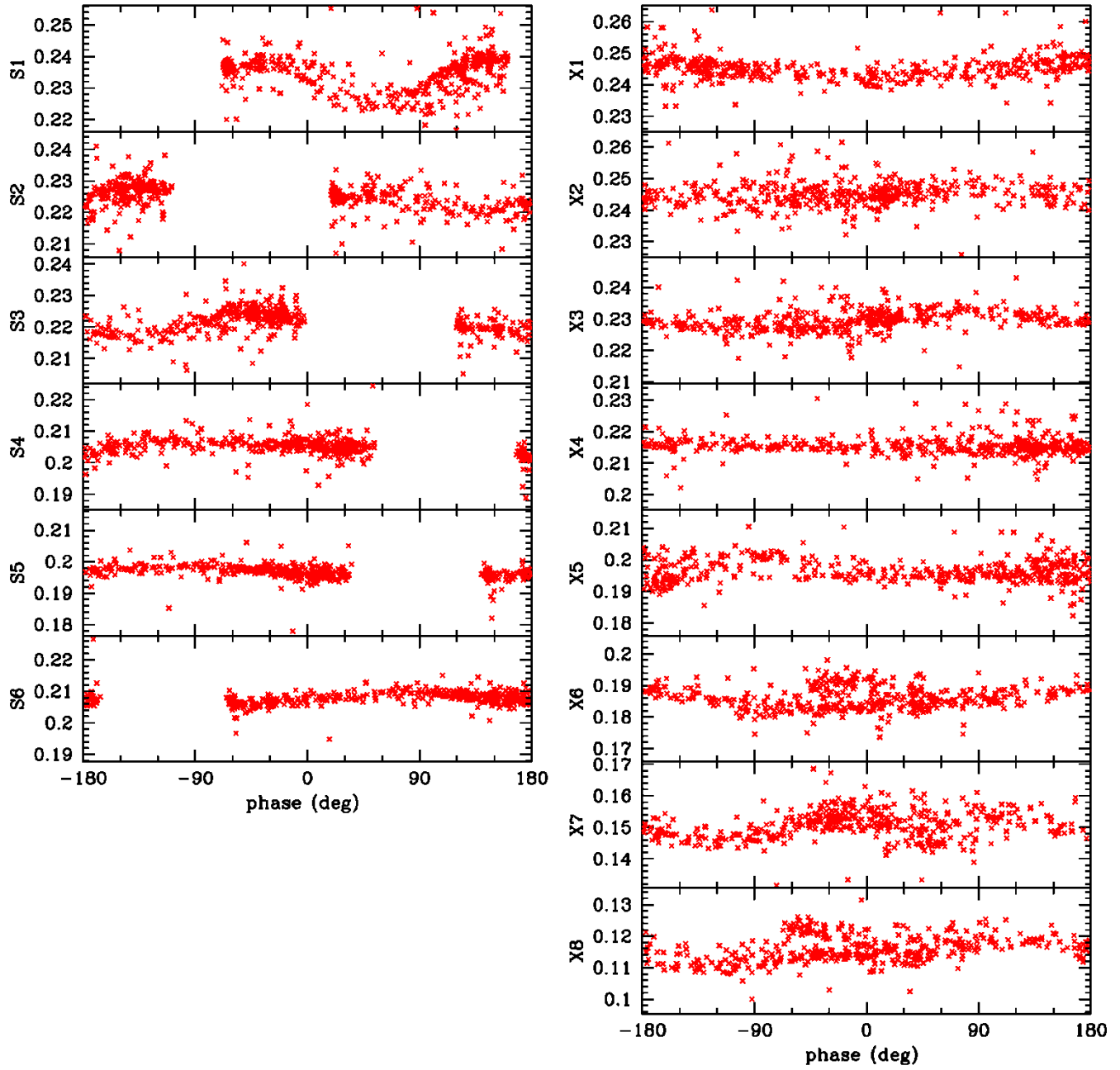


Figure 12. RD1707 S-band (left) and X-band (right) multitone pcal amplitudes vs. pcal phase, by channel.

Koee RD1707 pcal channel Tsys-normalized amplitude vs. phase



**Figure 13.** Same as Figure 12 except that each amplitude has been multiplied by the square root of the Tsys value in the Field System log..

Koee RD1707 pcal channel Tsys-normalized amplitude vs. channel-1 connected phase

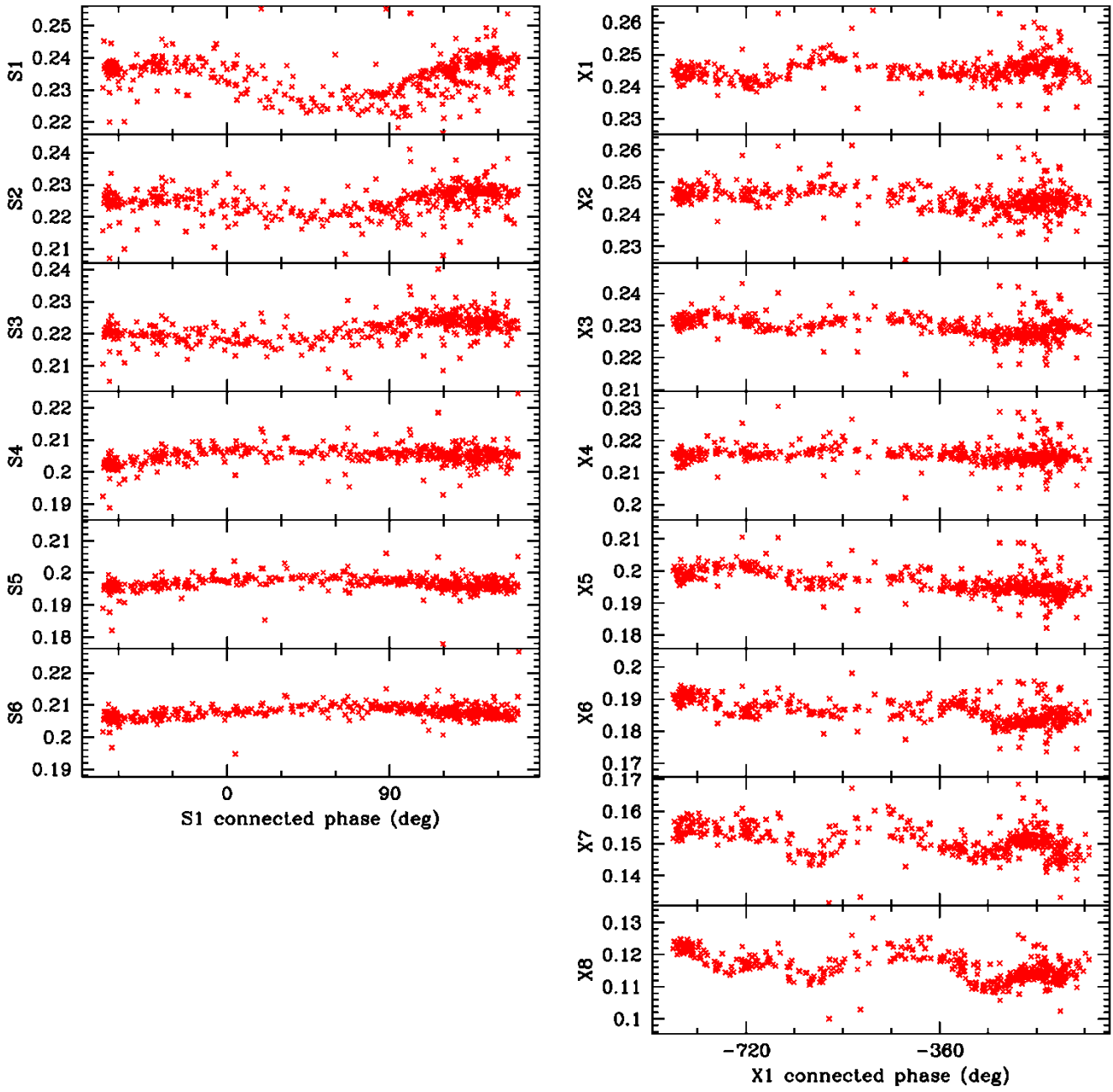


**Figure 14.** Same as Figure 13 except that now the abscissa is the connected phase in the lowest-frequency channel of the band.

Kokee RD1707 pcal channel amplitude ratio wrt mean over channels vs. connected pcal phase

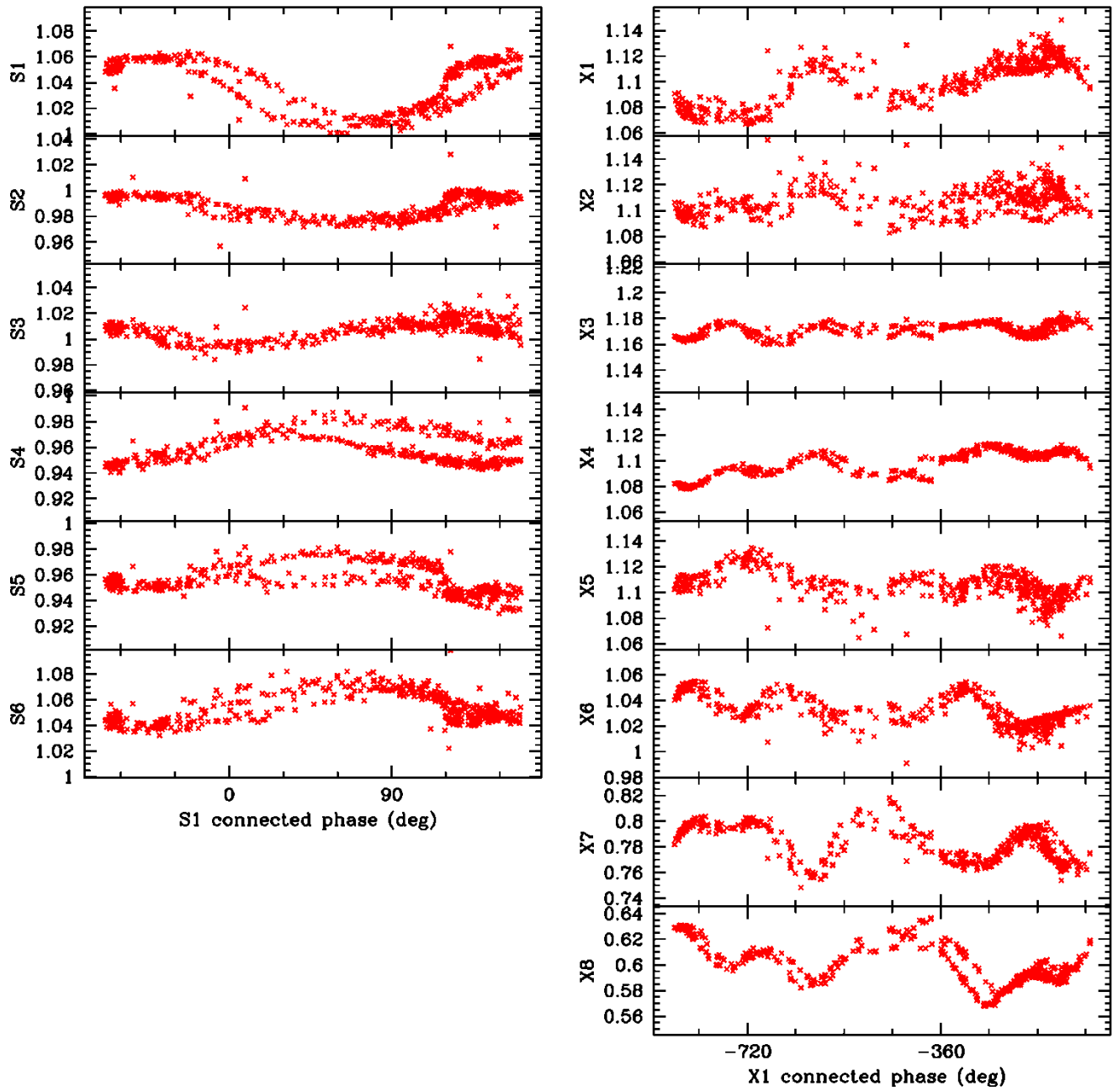


**Figure 15.** Same as Figure 14 except that now the ordinate is the multitone pcal amplitude of the channel divided by the mean amplitude across all channels in the band.

Koike RD1707 pcal phase residual to band model vs. channel-1 connected phase

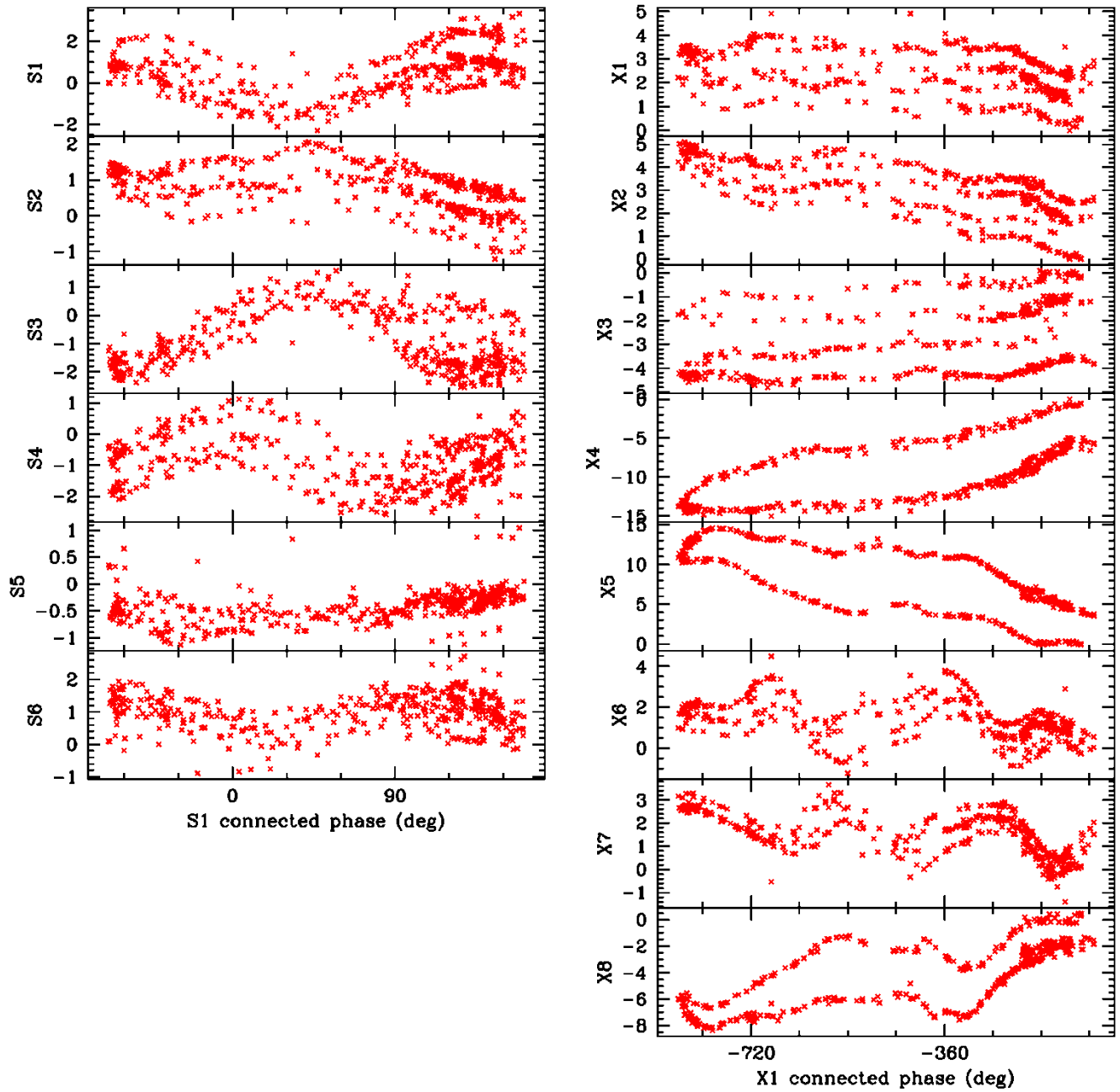


**Figure 16.** RD1707 S-band (left) and X-band (right) multitone pcal phase (deg), after subtracting the band model value from each phase, vs. connected phase in the lowest-frequency channel of the band.

### Kk RD1707 pcal amplitude vs. time

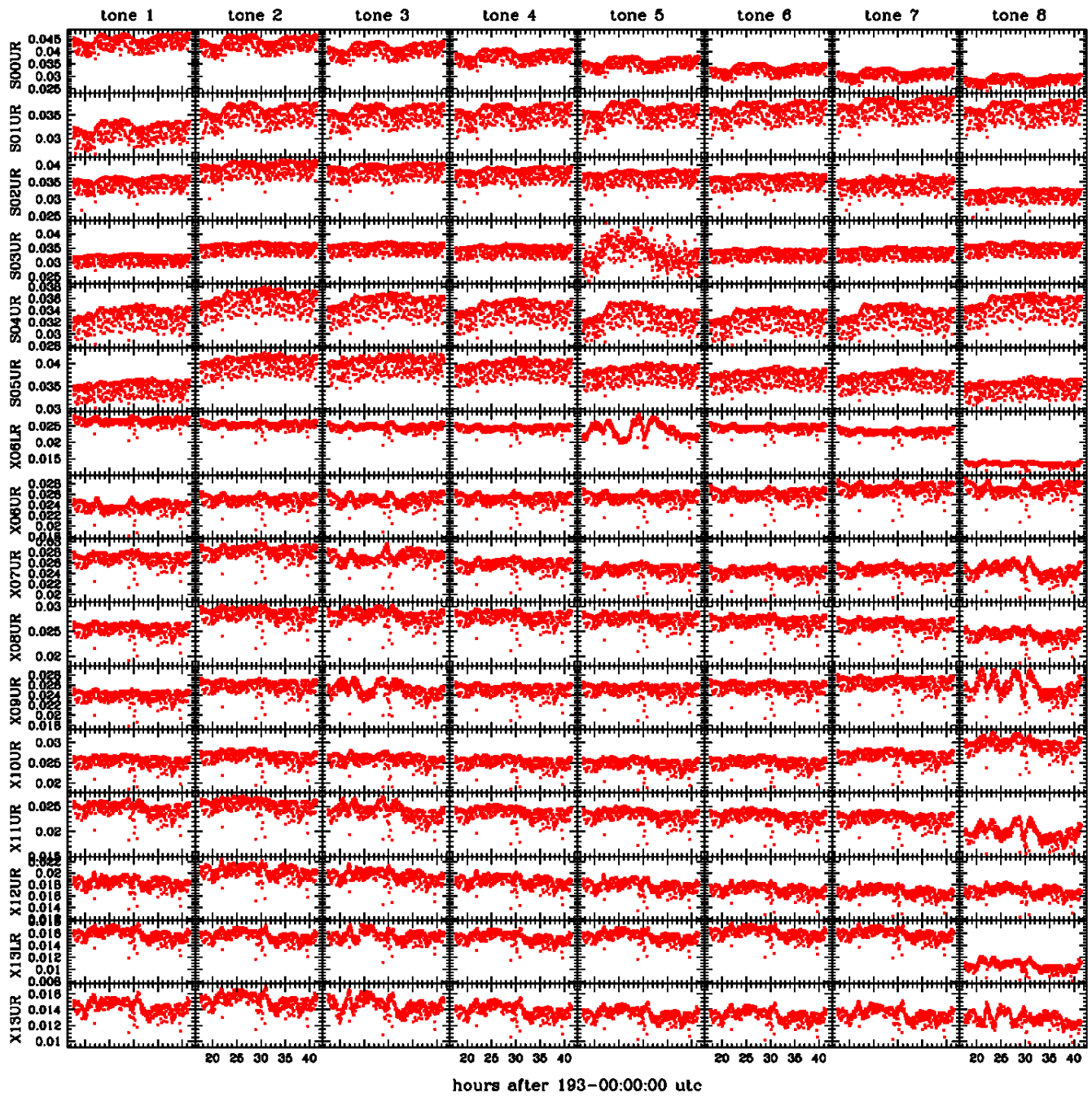


**Figure 17.** RD1707 pcal amplitude time series for individual pcal tones in all 16 channels / sidebands. The 8 tones in each sideband are displayed left to right, and the channels top to bottom. Tone 1 is the lowest frequency tone at baseband (0.010 MHz for USB), and tone 8 is the highest (7.99 MHz for USB).

Kk RD1707 pcal amplitude vs. phase

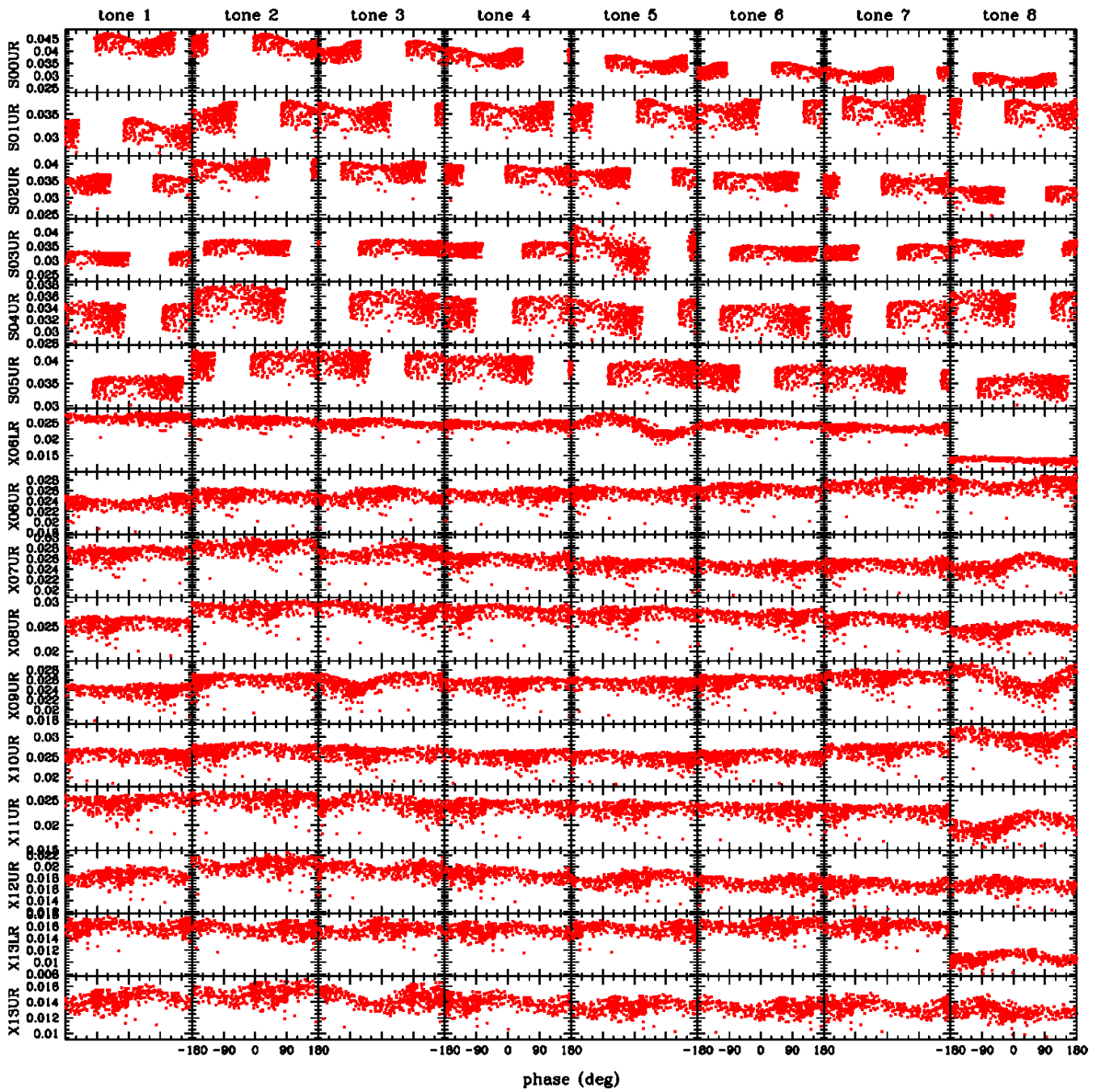


Figure 18. Same as Figure 17 except that now the abscissa is tone phase.

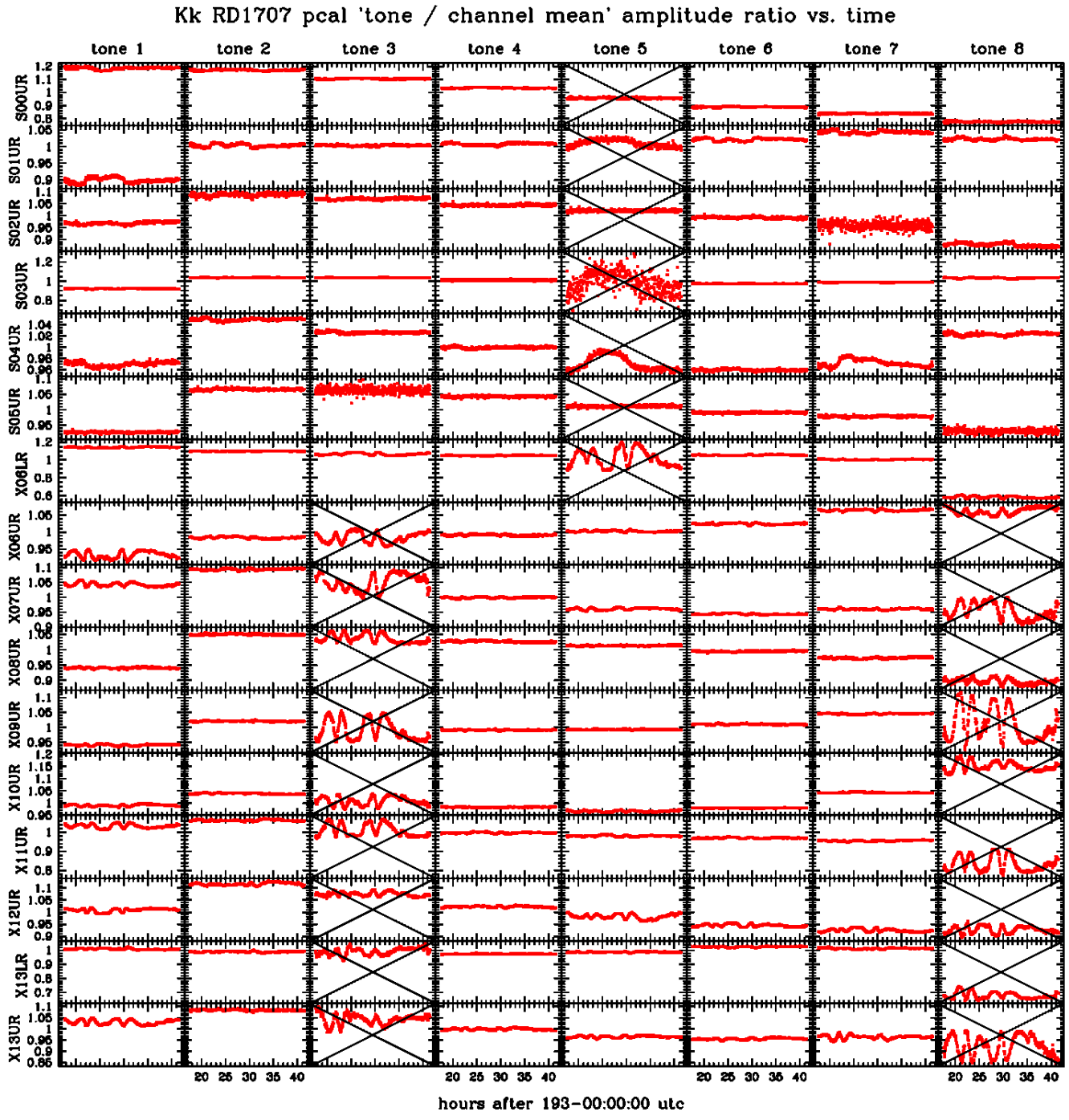


Figure 19. RD1707 pcal tone amplitude ratios between the amplitude of each tone and the mean amplitude over all unmasked tones in a given channel/sideband, vs. time. Masked-out tones are the 5<sup>th</sup> tone (4.01 MHz) in S-band USB channels, the 3<sup>rd</sup> and 8<sup>th</sup> tones (2.01 and 7.01 MHz) in X-band USB channels, and the 5<sup>th</sup> tone (4.99 MHz) in X06LR.

Kk RD1707 pcal 'tone / channel mean' amplitude ratio vs. phase

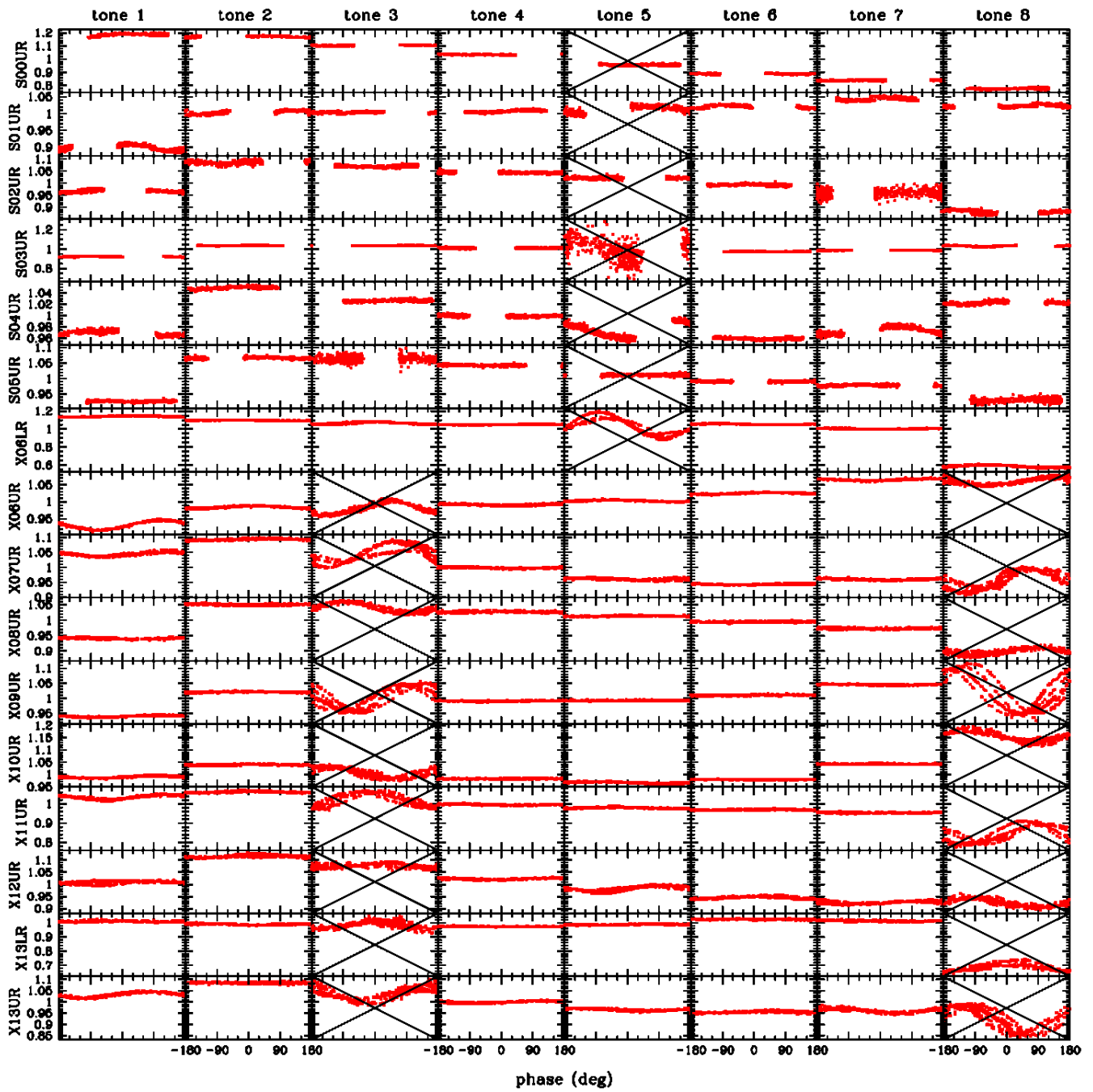
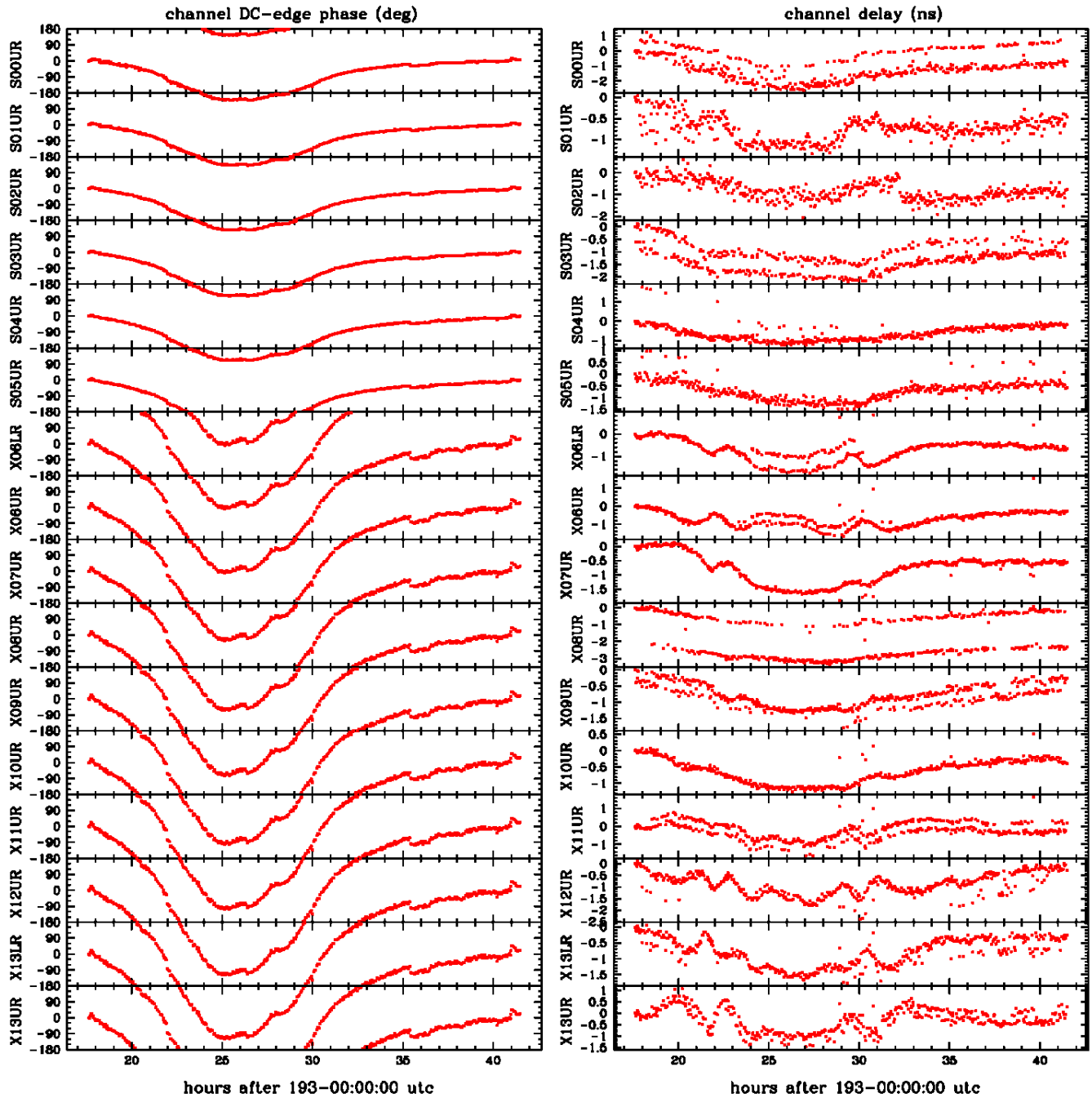
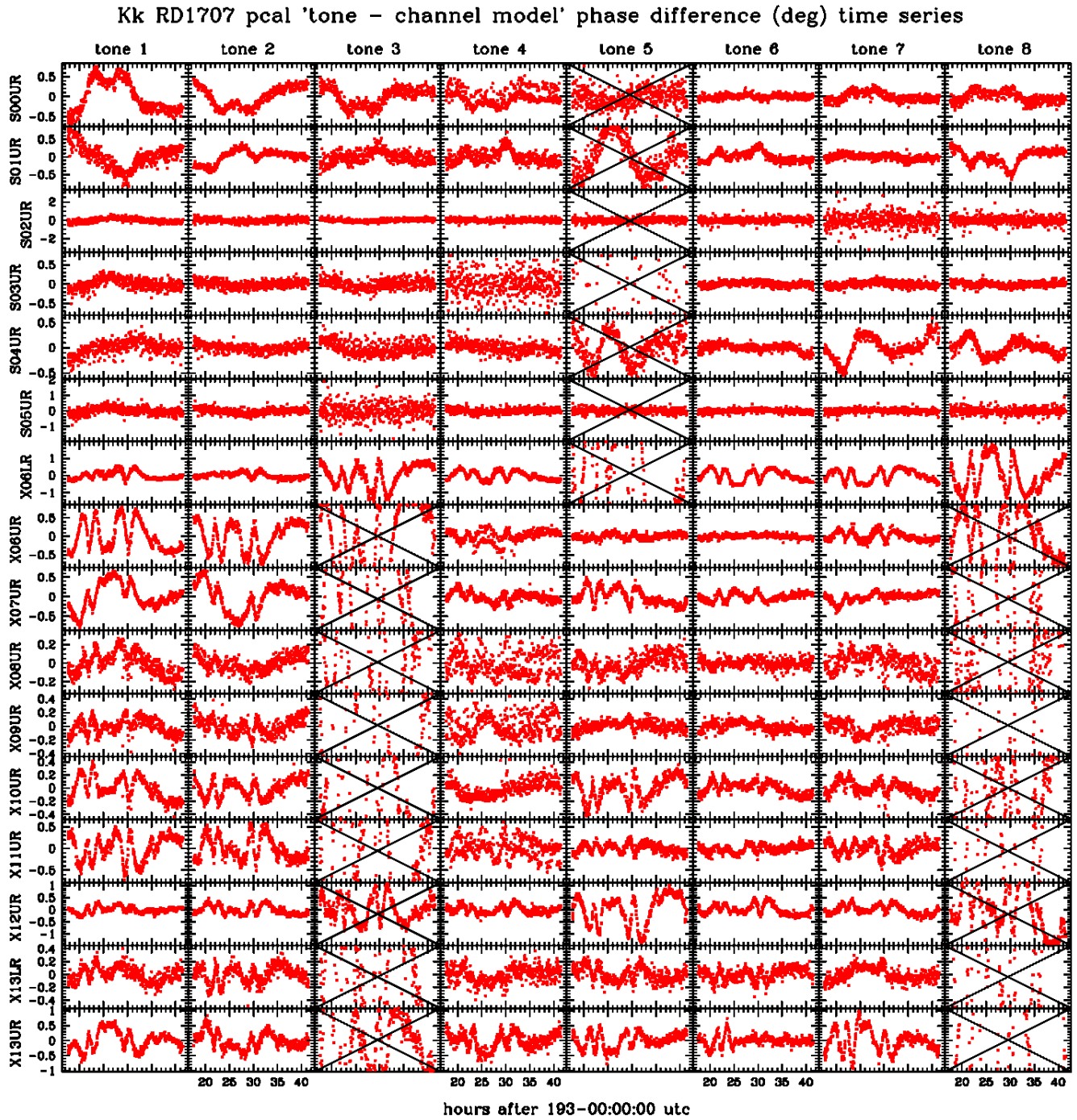


Figure 20. Same as Figure 19 except that now the abscissa is tone phase.

Kk RD1707 'masked' pcal channel model phase and delay time series



**Figure 21.** RD1707 channel model parameter time series for all 16 sidebands, with channel pcal phase (deg) at baseband DC edge on the left and channel pcal delay (ns) on the right. For each epoch and each sideband, a straight line is fit to tone phase vs. frequency, weighted by tone amplitude, for all tones not masked out. (Prior to fitting, the phase at the epoch of the first scan is subtracted from each tone phase time series.) Masked-out tones are the 5<sup>th</sup> tone (4.01 MHz) in S-band USB channels, the 3<sup>rd</sup> and 8<sup>th</sup> tones (2.01 and 7.01 MHz) in X-band USB channels, and the 5<sup>th</sup> tone (4.99 MHz) in X06LR.



**Figure 22.** RD1707 pcal tone phase differences between the phase of each tone and the channel model value for that tone, vs. time. Model value = (model DC-edge phase) + (model delay) x (baseband frequency), with model parameters shown in Figure 21.

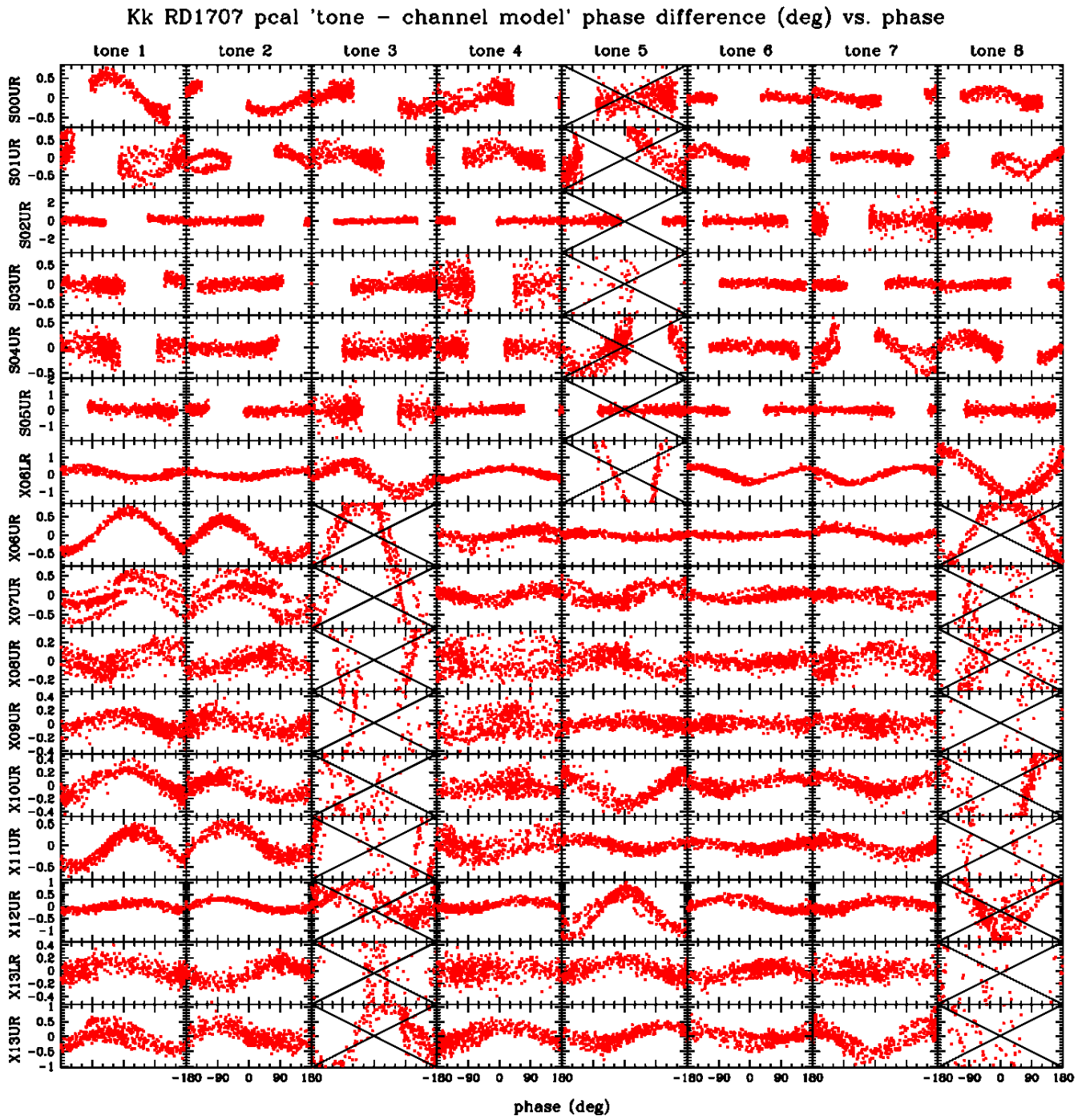
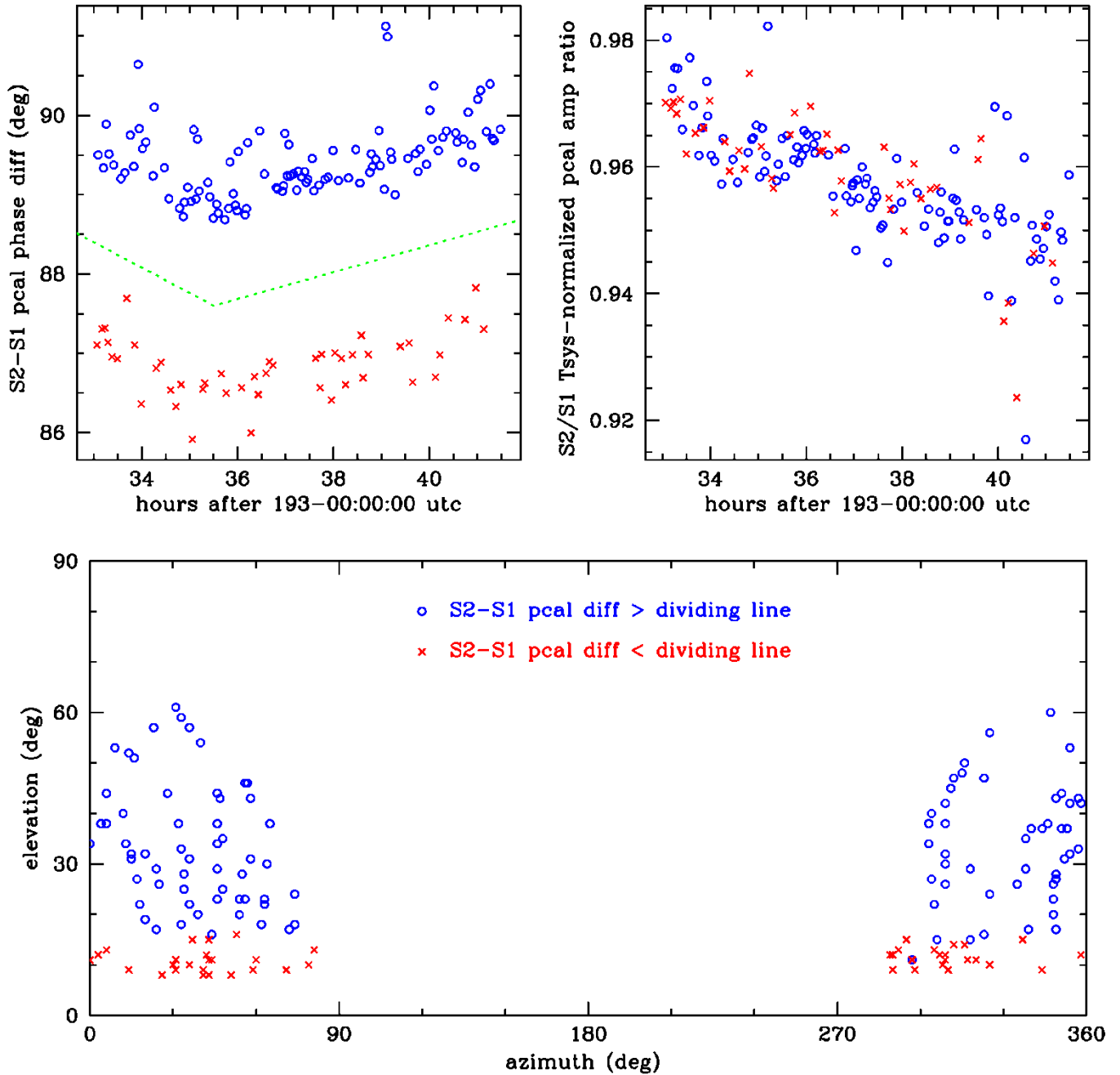


Figure 23. Same as Figure 22 except that now the abscissa is tone phase.

Kokee RD1707 S2-S1 pcal phase diff vs. az/el



**Figure 24.** RD1707 pcal behavior in channels S1 and S2 after 194-0900. Different plot symbols denote whether the S2-S1 phase difference is above or below the green dotted line in the top left panel. *Top left:* pcal phase difference vs. time. *Top right:* ratio between pcal amplitudes, each multiplied by sqrt(Tsys), vs. time. *Bottom:* scan elevation vs. azimuth.

RD1707 S2-S1 diffs for K pcal phase & KV fringe phase (K manual)

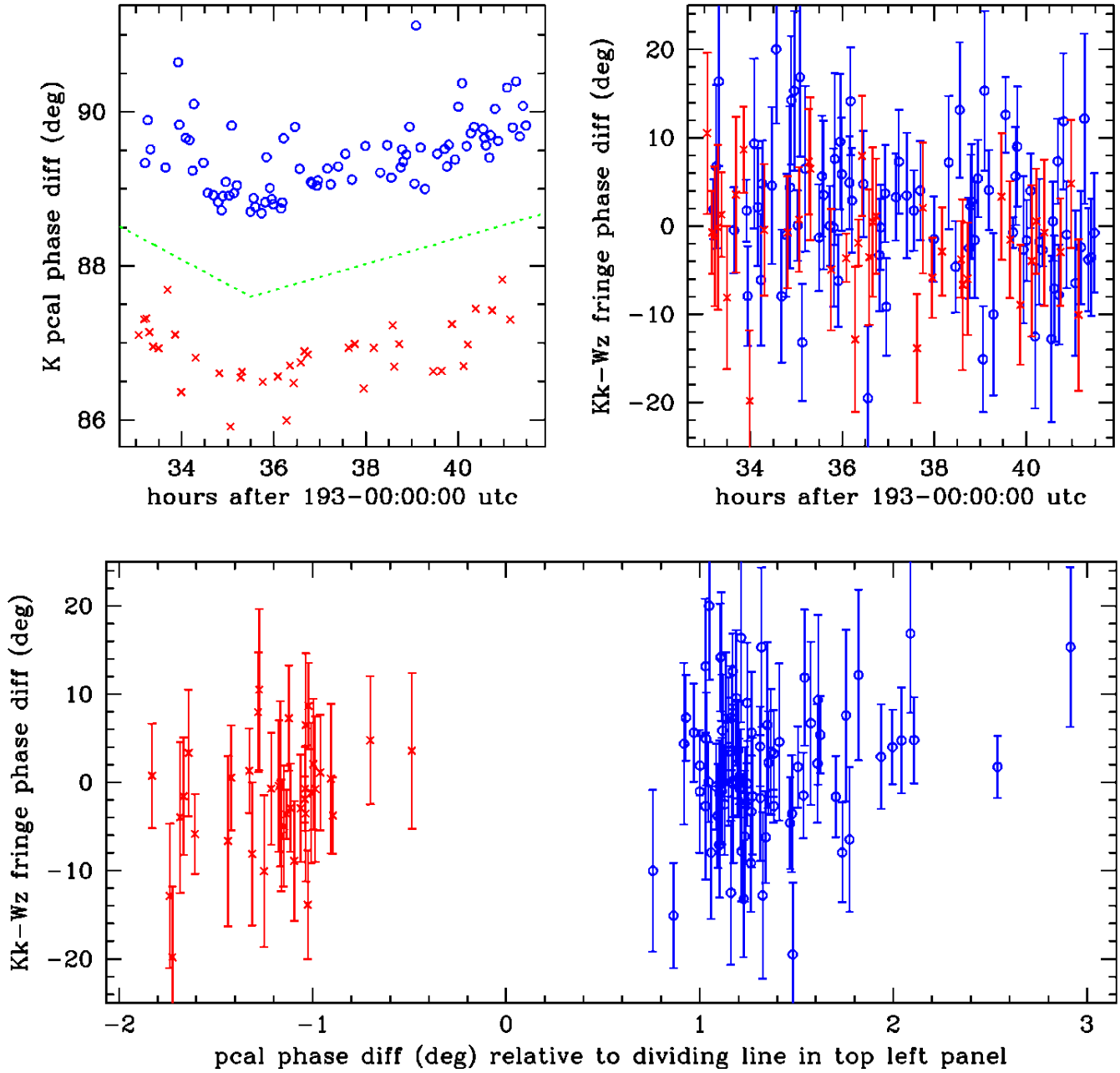


**Figure 25.** RD1707 pcal and residual fringe phase differences between channels S1 and S2 for scans after 194-0900 with SNR>20. Fringe phases are for KOKEE20M-WETTZELL baseline with Kokee fringed with **manual** phases. Different plot symbols denote whether the S2-S1 phase difference is above or below the green dotted line in the top left panel. *Top left:* pcal phase difference vs. time (same as top panel in Figure 24). *Top right:* fringe phase difference vs. time. *Bottom:* scan elevation vs. azimuth.

RD1707 S2-S1 diffs for K pcal phase & KV fringe phase (K multitone)

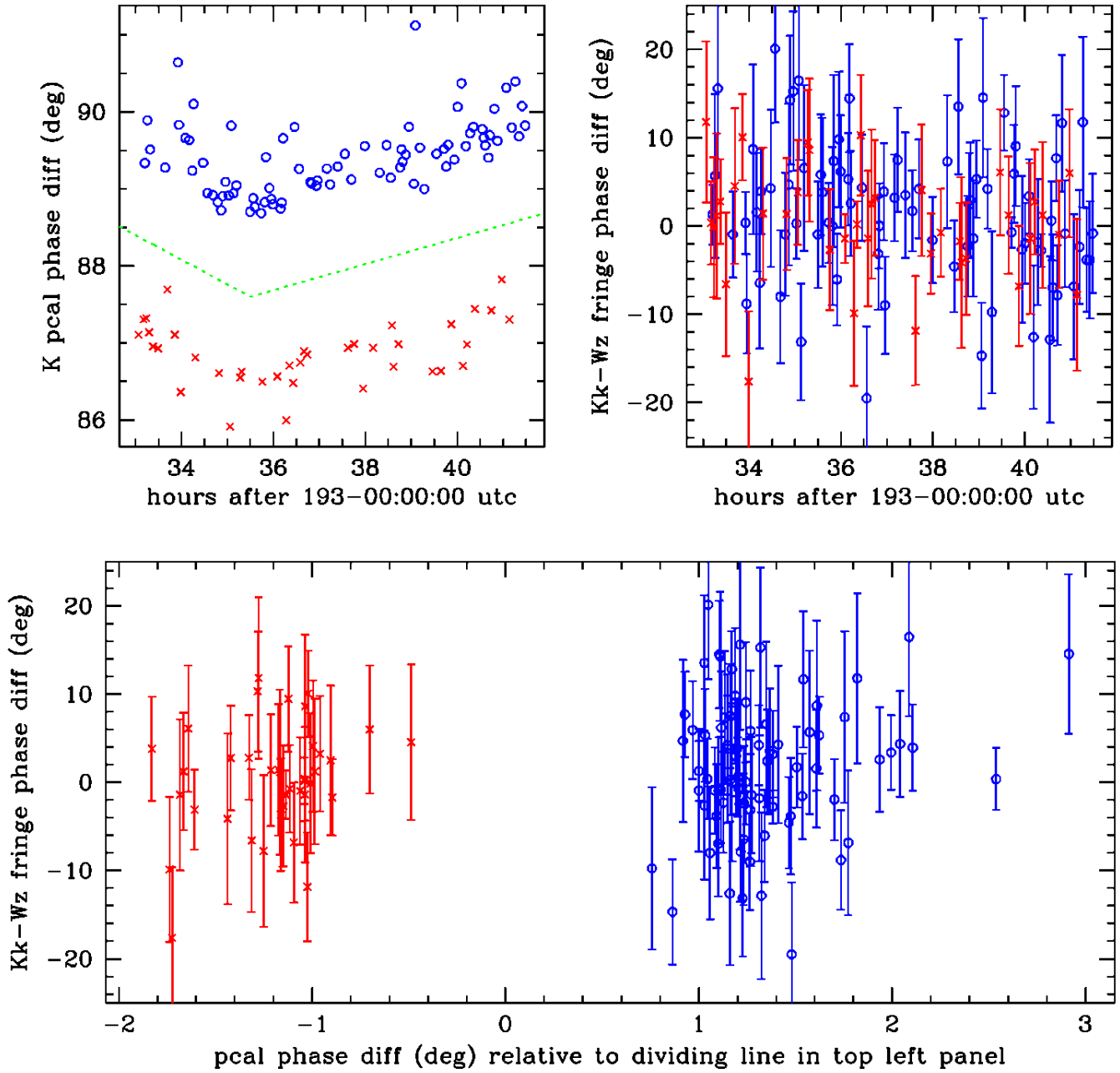
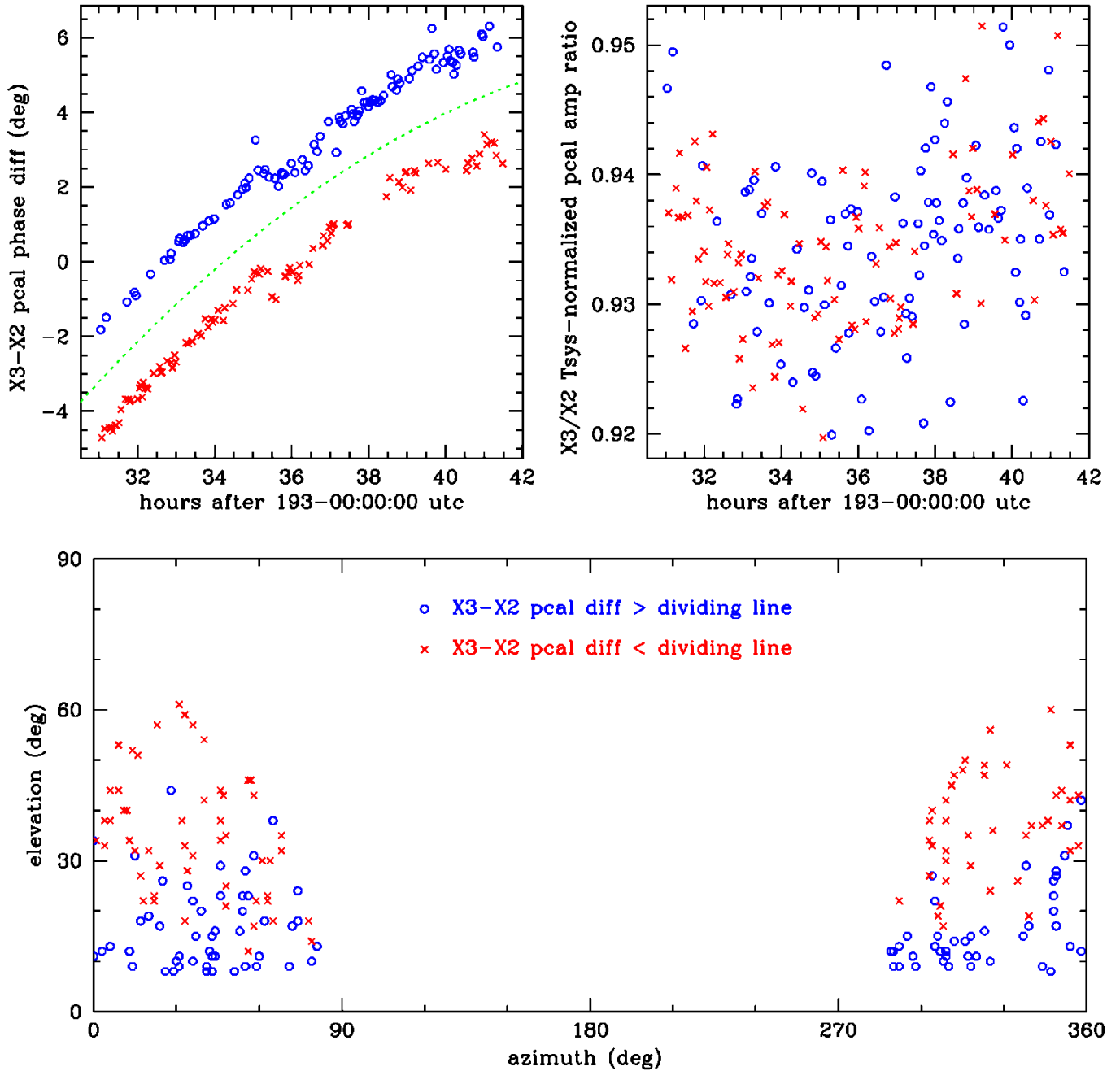


Figure 26. Same as Figure 25 except that Kokee was fringed with **multitone** pcal phases.

Kokee RD1707 X3-X2 pcal phase diff vs. az/el



**Figure 27.** RD1707 pcal behavior in channels X2 and X3 after 194-0700. Different plot symbols denote whether the X3-X2 phase difference is above or below the green dotted line in the top left panel. *Top left:* pcal phase difference vs. time. *Top right:* ratio between pcal amplitudes, each multiplied by  $\sqrt{T_{\text{sys}}}$ , vs. time. *Bottom:* scan elevation vs. azimuth.

RD1707 X3-X2 diffs for K pcal phase & KV fringe phase (K manual)

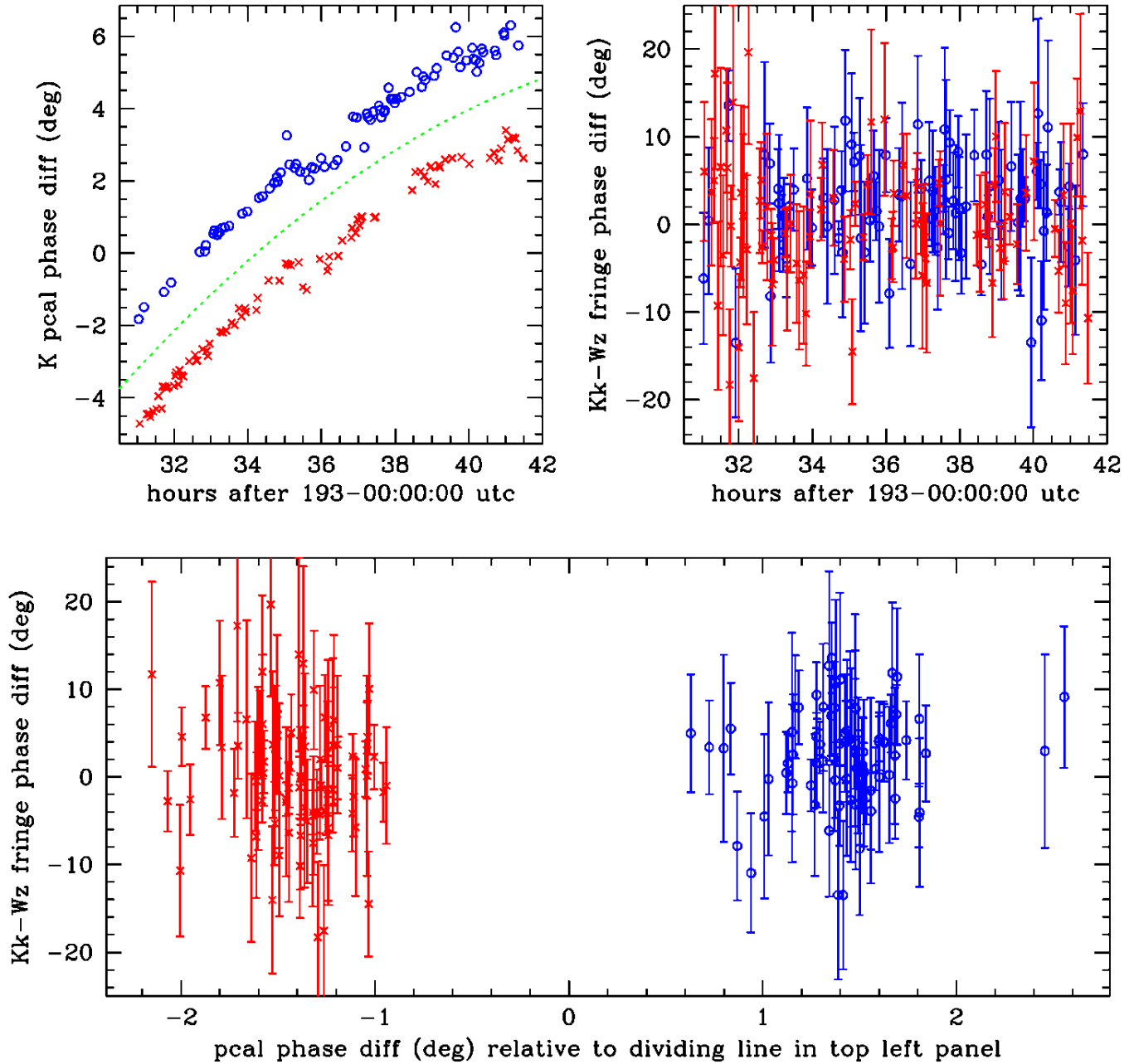


**Figure 28.** RD1707 pcal and residual fringe phase differences between channels X2 and X3 for scans after 194-0700 with SNR>20. Fringe phases are for KOKEE20M-WETTZELL baseline with Kokee fringed with **manual** phases. Different plot symbols denote whether the X3-X2 phase difference is above or below the green dotted line in the top left panel. *Top left:* pcal phase difference vs. time (same as top panel in Figure 27). *Top right:* fringe phase difference vs. time. *Bottom:* scan elevation vs. azimuth.

RD1707 X3-X2 diffs for K pcal phase & KV fringe phase (K multitone)

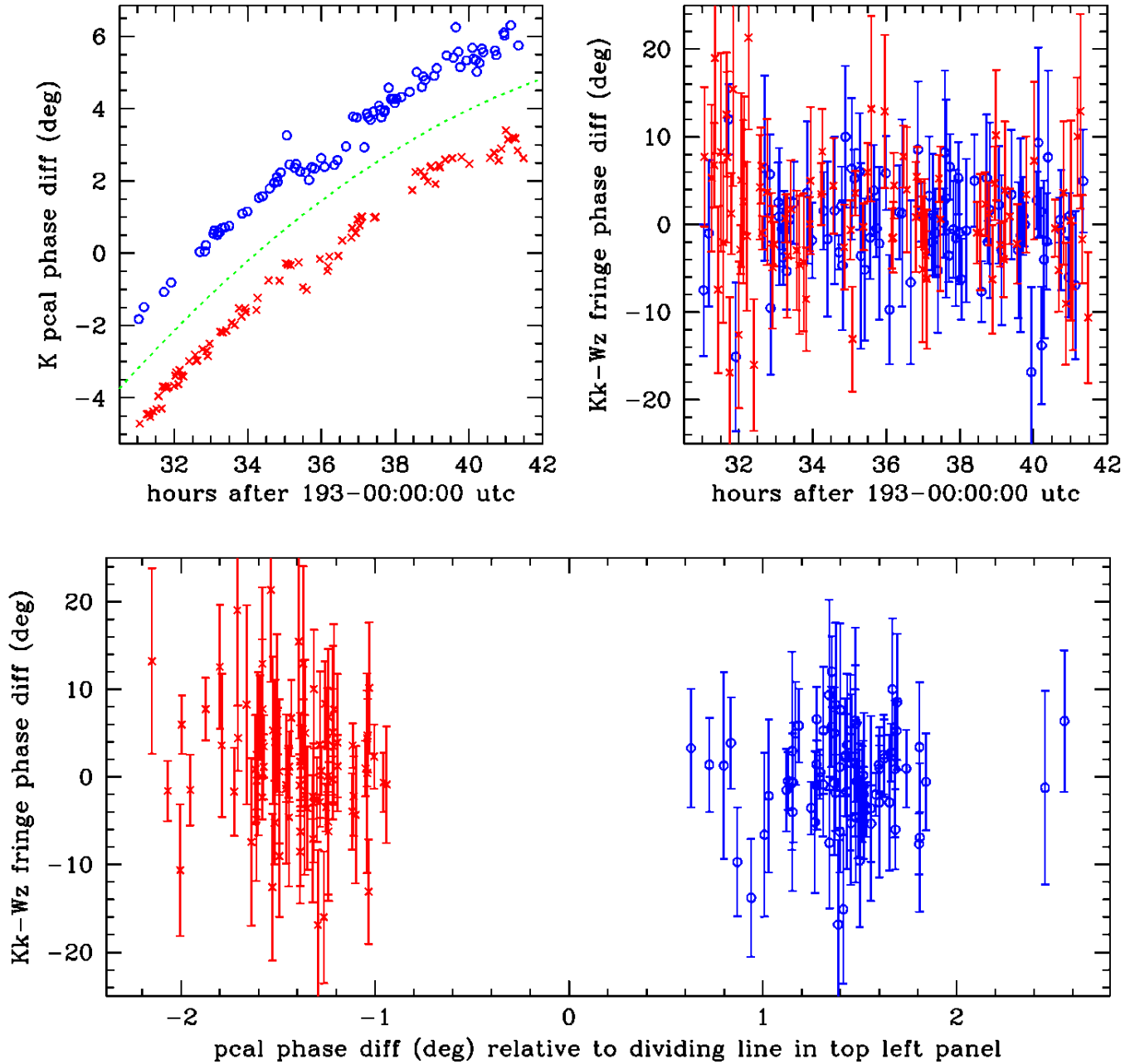


Figure 29. Same as Figure 28 except that Kokee was fringed with **multitone** pcal phases.

**Table 2.** Mean phase double differences from Figures 25, 26, 28, and 29.

Type of double difference	<i>S2-S1</i>	<i>X3-X2</i>
<i>pcal phase</i>	2.5°	2.8°
<i>fringe phase with Kk fringed with manual phases</i>	2.6° ± 1.1°	2.6° ± 0.7°
<i>fringe phase with Kk fringed with multitone phases</i>	0.4° ± 1.1°	-0.7° ± 0.7°

Explanation of table entries:

Define  $\Delta\phi_{pc,green}$  = difference between pcal phase difference (*S2-S1* or *X3-X2*) and dotted green dividing line in top left panel in figures. The values of  $\Delta\phi_{pc,green}$  clearly fall into 2 groups. Define data set *blue* to be scans for which  $\Delta\phi_{pc,green} > 0$  (blue circles in figures), and data set *red* to be scans for which  $\Delta\phi_{pc,green} < 0$  (red Xs in figures). Each entry in Table 2 is the mean over scans of the *blue-red* difference for the phase difference indicated. For example, the bottom righthand entry is the mean *blue-red* difference of *X3-X2* fringe phase differences with Kk fringed with multitone phases.

Kokee cable and pcal delay time series for RD1706, RD1707, and RD1804

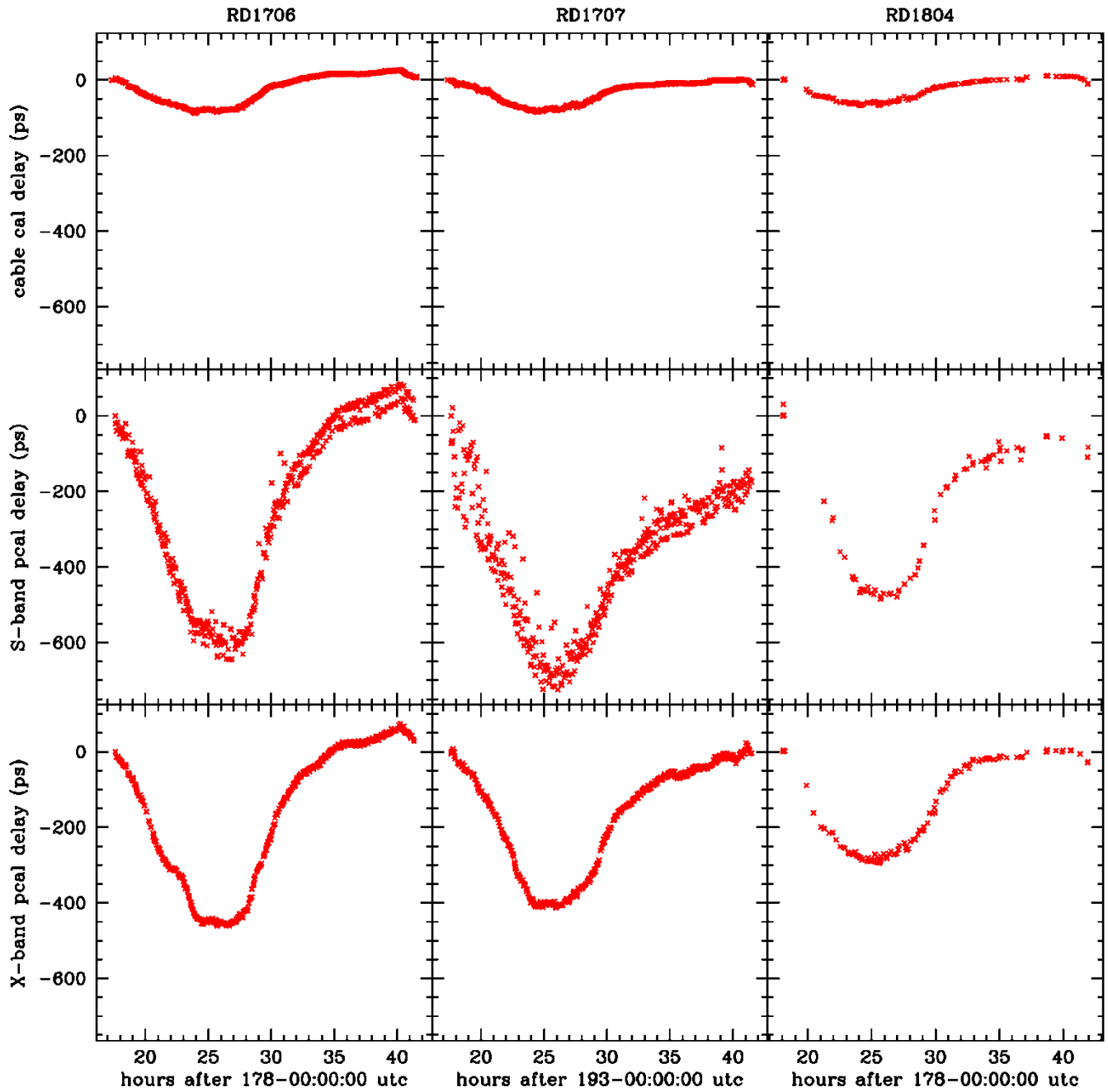


**Figure 30.** Top to bottom: cable cal delay, S-band pcal delay (for RD1707, same as band model delay in bottom panel of Figure 6), and X-band pcal delay (for RD1707, same as band model delay in bottom panel of Figure 7). Left to right: RD1706, RD1707, and RD1804 sessions.

Kokee RD1707 S/X pcal delay and cable delay vs az/el

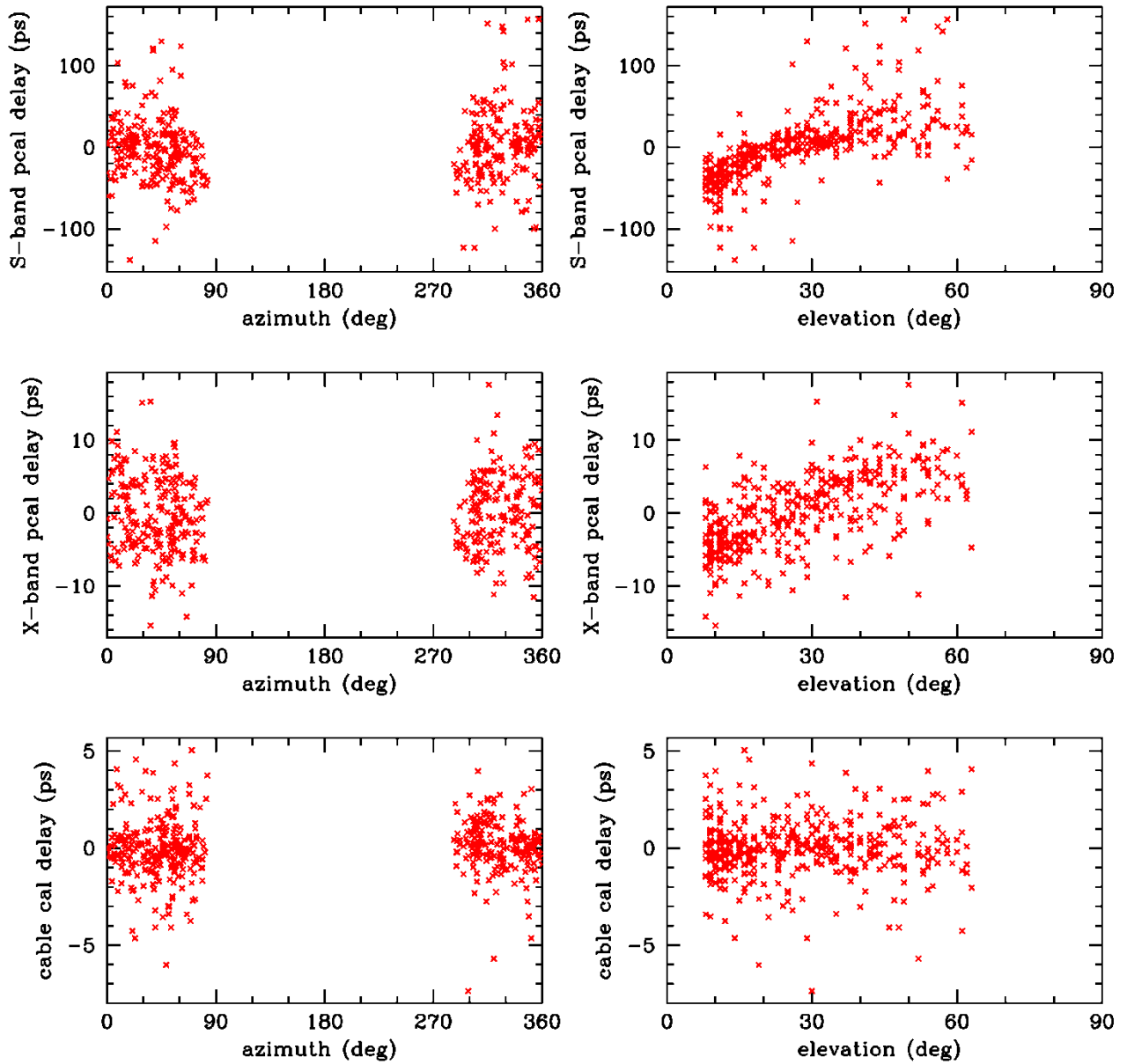


**Figure 31.** Top to bottom: RD1707 S-band pcal delay, X-band pcal delay, and cable cal delay vs. azimuth (left) and elevation (right). Data are residuals to points in middle column of Figure 30 after subtracting an 11-point running mean from each time series.

Kokee RD1804 S/X pcal delay and cable delay vs az/el

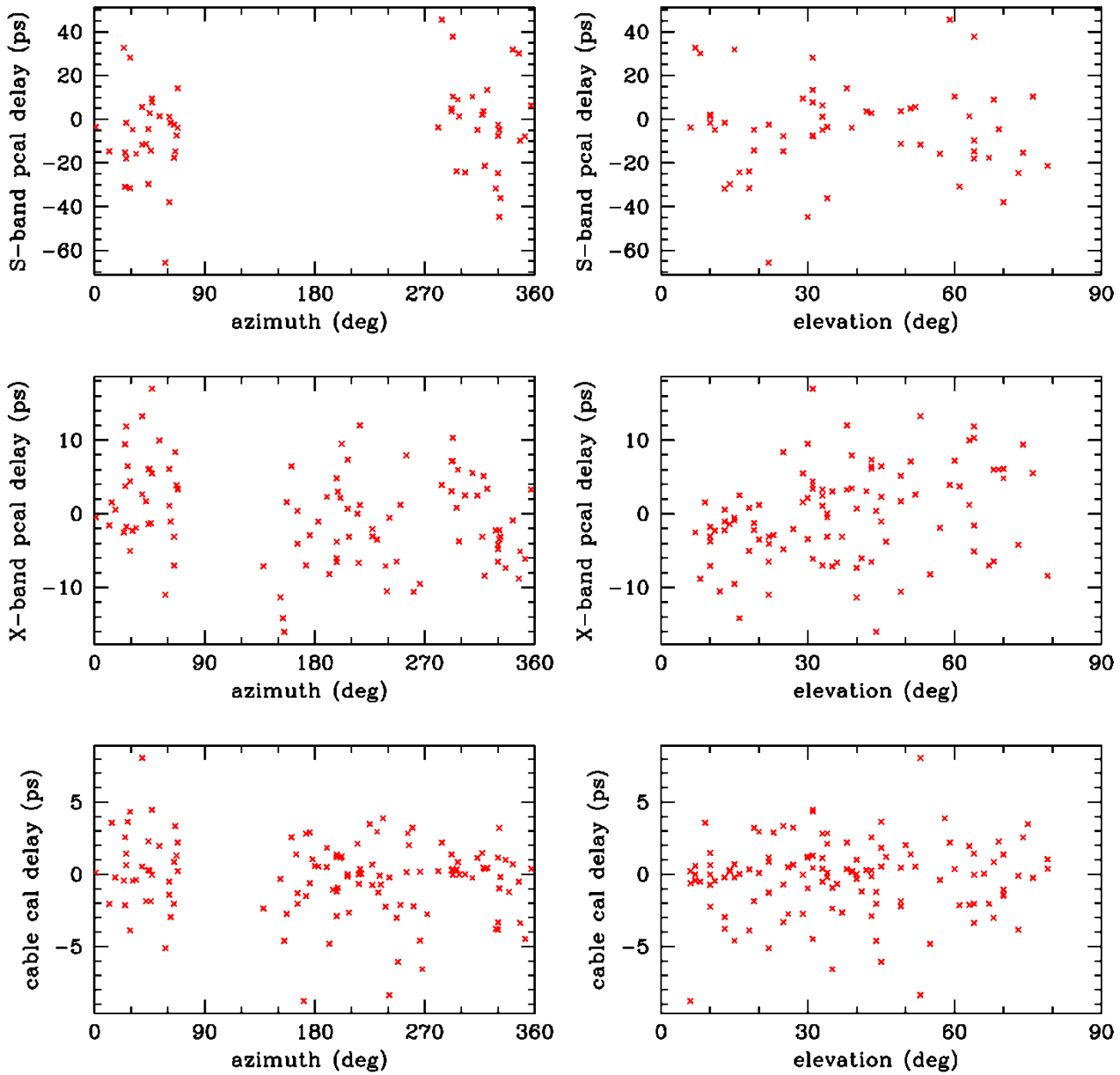


**Figure 32.** *Top to bottom:* RD1804 S-band pcal delay, X-band pcal delay, and cable cal delay vs. azimuth (*left*) and elevation (*right*). Data are residuals to points in righthand column of Figure 30 after subtracting an 11-point running mean from each time series. During RD1804, Kokee observations to the south were all with Hobart, for which the top 2 S-band channels were deleted in fringing due to RFI; the program that calculates pcal delay from the type-309 phases requires all channels be present, hence the large gap in azimuth coverage for S-band pcal delay.